

Fzd3 and *Fzd6* Deficiency Results in a Severe Midbrain Morphogenesis Defect

Sebastian Stuebner,^{1†} Theresa Faus-Kessler,¹ Thomas Fischer,¹ Wolfgang Wurst,^{1,2*} and Nilima Prakash^{1†}

Wnt/ β -catenin signaling controls the proper development of the mid-/hindbrain region (MHR) and of midbrain dopaminergic (mDA) neurons, but the Frizzled (Fzd) receptors transducing these signals are still unknown. *Fzd3* is expressed throughout the mouse anterior neural tube, whereas *Fzd6* is restricted to the MHR. We show that the MHR is properly established and mDA neurons develop normally in *Fzd6*^{-/-} mutants, but the number of mDA neurons is initially reduced and recovers at later stages in *Fzd3*^{-/-} embryos. *Fzd3*^{-/-}; *Fzd6*^{-/-} double mutants exhibit a severe midbrain morphogenesis defect consisting of collapsed brain ventricles, apparent thickening of the neuroepithelium, focal disruption of the ventricular basal lamina and protrusion of individual cells, and increased proliferation at later stages, despite a normal closure of the anterior neural tube and the rescue of the mDA defect in these embryos. *Fzd3* and *Fzd6* thus control proper midbrain morphogenesis by a yet unknown mechanism in the mouse. *Developmental Dynamics* 239:246–260, 2010. © 2009 Wiley-Liss, Inc.

Key words: Fzd3; Fzd6; Wnt1; midbrain; dopaminergic neurons; mouse; schizophrenia

Accepted 30 August 2009

INTRODUCTION

The Wnt (Wingless-related MMTV integration site) family of secreted, lipid-modified glycoproteins plays a fundamental role in many aspects of vertebrate and invertebrate development, including neural induction and patterning, cell proliferation, cell fate specification, cell polarization and migration, axon guidance, and synaptogenesis (Logan and Nusse, 2004; Ille and Sommer, 2005). The extracel-

lular Wnt molecules signal into the cell via three different pathways: the “canonical” Wnt/ β -catenin, and the “non-canonical” Wnt/planar cell polarity (PCP) and Wnt/ Ca^{2+} pathways (Seifert and Mlodzik, 2007; Huang and He, 2008). Common to all three pathways is the binding of the Wnt ligand to the seven-pass transmembrane receptors of the Frizzled (Fzd) family, although Wnts can also bind to other single transmembrane recep-

tors (Huang and Klein, 2004; van Amerongen et al., 2008). The subsequent activation of one of the three signaling pathways appears to depend on the specific complement of Fzd receptors and co-receptors of the Low density lipoprotein (LDL) receptor-related protein (Lrp) family encountered on the surface of the receiving cell rather than on the Wnt ligand activating these receptors (van Amerongen et al., 2008). However,

Additional Supporting Information may be found in the online version of this article.

¹Institute of Developmental Genetics, Helmholtz Centre Munich, German Research Centre for Environmental Health, and Technical University Munich, Deutsches Zentrum für Neurodegenerative Erkrankungen (DZNE), Munich/Neuherberg, Germany

²Max Planck Institute of Psychiatry, Munich, Germany

Grant sponsor: Federal Ministry of Education and Research (BMBF) in the framework of the National Genome Research Network (NGFN+ Functional Genomics of Parkinson's Disease); Grant number: FKZ 01GS08174. Grant sponsor: Virtual Institute of Neurodegeneration and Ageing; Grant number: VH-VI-252. Grant sponsor: Initiative and Networking Fund in the framework of the Helmholtz Alliance of Systems Biology and of Mental Health in an Ageing Society; Grant number: HA-215. Grant sponsor: Bayerischer Forschungsverbund “ForNeuroCell”; Grant number: F2-F2410-10c/20697. Grant sponsor: European Union mdDANEURODEV; Grant number: FP7-Health-2007-B-222999. Grant sponsor: European Union EuTRACC; Grant number: LSHG-CT-2006-037445. Grant sponsor: Deutsche Forschungsgemeinschaft (DFG); Grant numbers: SFB 596, WU 164/3-2, WU 164/4-1.

[†]Sebastian Stuebner and Nilima Prakash contributed equally to this work.

*Correspondence to: Wolfgang Wurst, Helmholtz Centre Munich, German Research Centre for Environmental Health, Institute of Developmental Genetics, Ingolstaedter Landstr. 1, D-85764 Neuherberg, Germany. E-mail: wurst@helmholtz-muenchen.de

DOI 10.1002/dvdy.22127

Published online 19 October 2009 in Wiley InterScience (www.interscience.wiley.com).

the identification of the individual Wnt/Fzd ligand/receptor pairs acting during the development of higher vertebrates has been complicated enormously by the fact that 19 Wnt ligands face 10 Fzd receptors encoded in the mammalian genome, thus allowing for potentially 190 different ligand/receptor pair combinations (van Amerongen et al., 2008).

The hallmark of the Wnt/ β -catenin pathway is the stabilization of cytosolic β -catenin, which subsequently enters the cell nucleus and activates the transcription of Wnt target genes (Huang and He, 2008). Apart from many other developmental processes in the mouse, the Wnt/ β -catenin pathway is required for the maintenance of the isthmus organizer (IsO) at the mid-/hindbrain boundary (MHB), a key signaling center that controls the proper development of the midbrain and rostral hindbrain in the mouse embryo (Braut et al., 2001; Wurst and Bally-Cuif, 2001). More recent data also indicate that the generation of dopamine-synthesizing (dopaminergic, DA) neurons in the ventral midbrain (VM), a very important neuronal population controlling motor behaviors and cognitive and affective brain functions, crucially relies on the activation of the Wnt/ β -catenin pathway in their progenitors (Joksimovic et al., 2009; Tang et al., 2009). Due to the phenotypic resemblances of the corresponding mouse mutants, Wnt1 appears to be the Wnt ligand activating this pathway in both cases, although the participation of other Wnts cannot be completely ruled out (McMahon and Bradley, 1990; Thomas and Capecchi, 1990; Prakash et al., 2006). The identity of the Fzd receptors transducing the Wnt1 signal at the MHB and in midbrain dopaminergic (mDA) progenitors, however, still remains to be established. To this end, we have performed a detailed analysis of the mouse Fzd expression patterns at the MHB and in the cephalic flexure (the site of origin of mDA neurons) during midgestational stages of embryonic development (Fischer et al., 2007). This analysis revealed a striking pattern of *Fzd6* expression in the caudal cephalic flexure and at the MHB in the developing mouse embryo (Fischer

et al., 2007). We, therefore, hypothesized that the *Fzd6* receptor might be a strong candidate to transduce the Wnt1 signal at these sites, although it might function in a redundant manner with the ubiquitously expressed *Fzd3* receptor (Fischer et al., 2007).

To establish a function of *Fzd6* and *Fzd3* in mid-/hindbrain and mDA neuron development, we analyzed the development of these regions and neuronal populations in *Fzd6*^{-/-} and *Fzd3*^{-/-} single and double mutant mouse embryos. *Fzd6*^{-/-} single mutants display hair-patterning defects, but a central nervous system (CNS) phenotype has not been reported in these mutant mice (Guo et al., 2004). *Fzd3*^{-/-} single mutants, by contrast, have strong defects in commissural axon projection in the spinal cord and lack all major fiber tracts in the forebrain including the DA nigrostriatal projections, although mDA neurons still arise in these mutants (Wang et al., 2002; Lyuksyutova et al., 2003). The cephalic neural tube closure defect observed with a low penetrance in the *Fzd3*^{-/-} single mutants (Wang et al., 2002), was reported to become a fully open neural tube with almost 100% penetrance in the *Fzd3*^{-/-}; *Fzd6*^{-/-} double mutants (Wang et al., 2006a). We show here that *Fzd6* is not required for transduction of the Wnt1 signal at the MHB and in mDA progenitors, as the IsO was established correctly at the MHB and mDA neurons developed normally in the VM of *Fzd6*^{-/-} single mutant mouse embryos. Notably, and although the MHB appeared morphologically normal in the *Fzd3*^{-/-} single mutants, the number of mDA neurons was transiently reduced in these mutants at midgestation. Because cell proliferation and survival was not affected in the *Fzd3*^{-/-} VM, this suggests that *Fzd3* is required for the proper differentiation of mDA neurons. In addition, we describe a severe midbrain morphogenesis defect in the *Fzd3*^{-/-}; *Fzd6*^{-/-} double mutants consisting of a normal closure of the anterior neural tube but collapse of all brain ventricles together with an apparent thickening of the neuroepithelium. The focal disruption of the ventricular basal lamina and protrusion of individual cells, together with an increased proliferation in the double

mutant midbrain at later stages, probably led to the massive protrusion of neural tissue and occlusion of the ventricular cavity of the midbrain observed in some double mutants. The increased proliferation in the *Fzd3*^{-/-}; *Fzd6*^{-/-} VM most likely also rescued the *Fzd3*^{-/-} mDA phenotype, as the mDA neuron numbers were not significantly altered in the double mutants. This double mutant phenotype is different from the previously reported neural tube closure defects in the *Fzd3*^{-/-} single and *Fzd3*^{-/-}; *Fzd6*^{-/-} double, and other Wnt/PCP pathway mutants (Copp et al., 2003; Wang et al., 2006a), and has to the best of our knowledge not been reported in the literature so far.

RESULTS

Fzd6 Is Expressed in *Wnt1*⁺ Cells at the MHB and in *Aldh1a1*⁺ mDA Precursors

The starting point of our analyses was the finding of a highly restricted expression of the *Fzd6* receptor in the caudal midbrain just abutting the MHB (Fig. 1) (Fischer et al., 2007). This *Fzd6* expression domain appeared to overlap with *Wnt1*, one of the key IsO genes required for the proper development of the midbrain and rostral hindbrain (McMahon and Bradley, 1990; Thomas and Capecchi, 1990; Fischer et al., 2007). Moreover, mDA neurons develop from *Wnt1*⁺ and *Aldh1a1*⁺ (*Aldehyde dehydrogenase family 1, subfamily a1*; also known as *Raldh1* or *Ahd2*) progenitors located in the ventral midline of the midbrain (Wallen et al., 1999; Zervas et al., 2004; Kittappa et al., 2007; Ono et al., 2007), the so-called floor plate (FP), and *Wnt1* and the Wnt/ β -catenin pathway are both necessary and sufficient for the generation of mDA neurons from the midbrain FP (Prakash et al., 2006; Joksimovic et al., 2009; Tang et al., 2009). Therefore, we first mapped in more detail the expression of *Fzd6* in relation to these two marker genes, *Wnt1* and *Aldh1a1*, at three crucial stages during the development of the mid-/hindbrain region (MHR) and of mDA neurons. The activity and gene expression patterns of the IsO are fully established at E10.5 (Wurst and

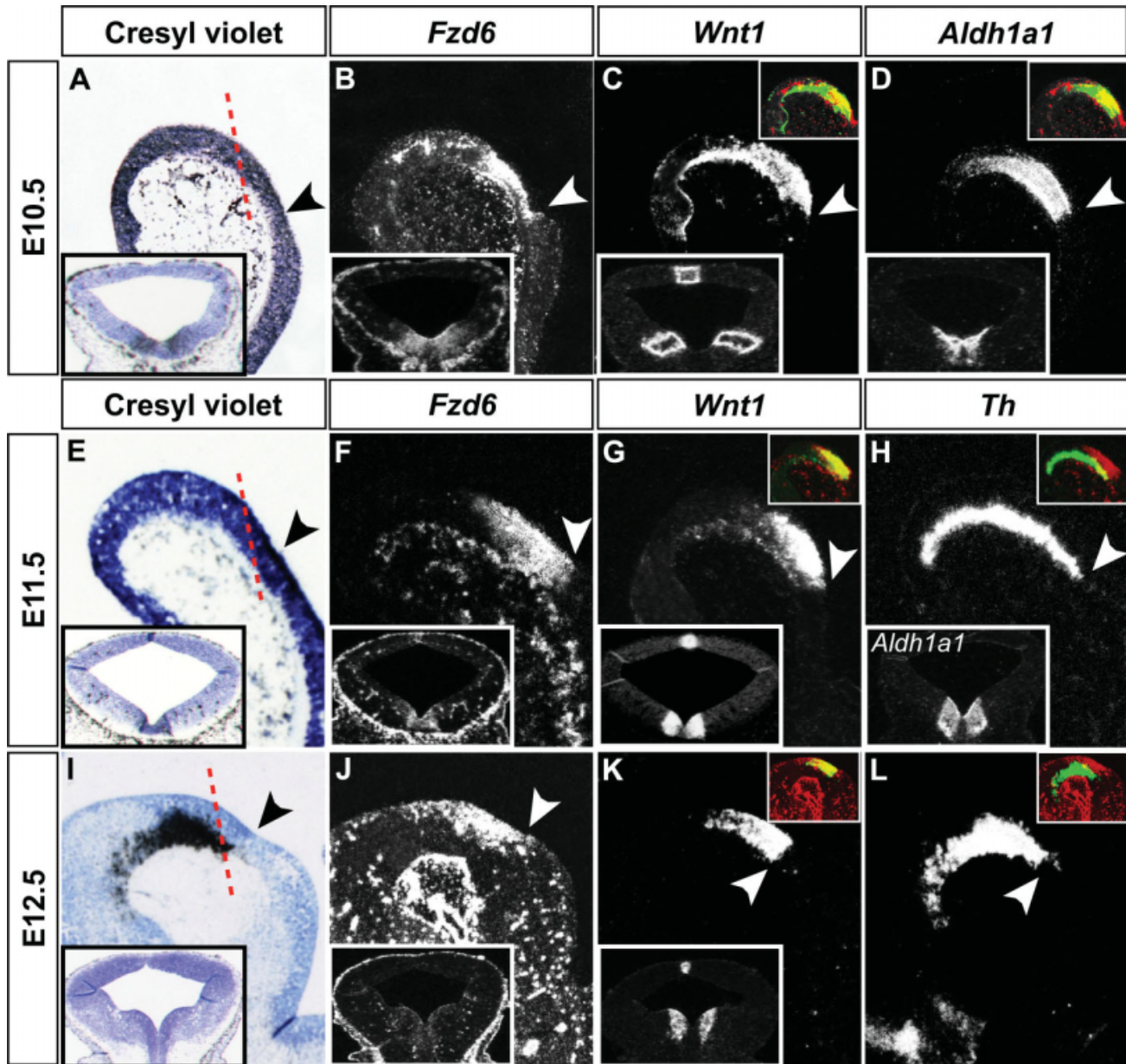


Fig. 1. Expression of *Fzd6* overlaps with *Wnt1* and *Aldh1a1* in the cephalic flexure of midgestational mouse embryos. A–L: Representative close-up views of the cephalic flexure in midsagittal sections from E10.5 (A–D), E11.5 (E–H), and E12.5 (I–L) CD-1 mouse embryos hybridized with riboprobe for *Fzd6* (B,F,J), *Wnt1* (C,G,K), *Aldh1a1* (D and inset in H), and *Th* (H,L). Dorsal is at the top, anterior to the left. A,E,I are brightfield images of D,H,L. Red broken lines in A,E,I indicate the plane of coronal sections at caudal midbrain levels shown in the bottom left corner insets in A–K. Black (A,E,I) and white (B–D,F–H,J–L) arrowheads point at the ventral position of the MHB. Top right corner insets in C,D,G,H,K,L are pseudo-colored overlays of consecutive sagittal sections hybridized with *Fzd6* (red) and *Wnt1* (green in C,G,K), *Aldh1a1* (green in D), or *Th* (green in H,L); overlapping expression domains appear in yellow.

Bally-Cuif, 2001). Moreover, most mDA neurons are born at an equivalent stage in the rat embryo (Gates et al., 2006), but only very few cells express Tyrosine hydroxylase (*Th*), the rate-limiting enzyme in DA synthesis, at E10.5 in the mouse embryo. As reported before, *Fzd6* expression is localized to the caudal cephalic flexure abutting the MHB ventrally at E10.5 (Fig. 1B), where it overlaps to a

large extent with *Wnt1* and *Aldh1a1* expression (Fig. 1C,D). *Fzd6* and *Aldh1a1* expression also overlap in a dorsoventral (D/V) and medio-lateral position at this stage, i.e., both genes are expressed strongly in the lateral FP and basal plate (BP) of the midbrain but weakly in the medial FP (insets in Fig. 1B,D). *Wnt1*, by contrast, is expressed in two stripes within the BP and lateral FP abutting

the medial FP and thus overlapping only partially with *Fzd6* expression (insets in Fig. 1B,C). *Fzd6* is not expressed in the dorsal midbrain (DM) at this stage (inset in Fig. 1B) (Fischer et al., 2007). A similar confinement of *Fzd6* transcription to the caudal cephalic flexure and overlap with *Wnt1* or *Aldh1a1* expression in this region is seen at E11.5 and E12.5 (Fig. 1F,G,J,K and inset in Fig. 1H),

when mDA precursors start to differentiate into mature Th⁺ mDA neurons, although the main patterning activity of the IsO might have already ceased at these stages (Wurst and Bally-Cuif, 2001; Ang, 2006). Notably, *Fzd6* expression only overlaps with a caudal subset of postmitotic Th⁺ mDA neurons at E11.5 and not at all with these neurons at E12.5 (colored insets in Fig. 1H,L).

We concluded from these analyses that *Fzd6* is expressed at crucial stages in *Aldh1a1*⁺ mDA progenitors and within at least a subset of, and in close vicinity to, *Wnt1*⁺ neuroepithelial cells at the MHB. The *Fzd6* receptor might, thus, transduce the Wnt1 signal required for the development of the midbrain and of associated neuronal populations such as the mDA neurons.

Establishment of the IsO at the MHB and the Development of mDA Neurons Are Not Affected in *Fzd6*^{-/-} Mutant Embryos

Based on the previous results, we first investigated whether the loss of the *Fzd6* receptor in *Fzd6*^{-/-} null mutants leads to a defective establishment of the MHB and/or patterning of the MHR at midgestational stages. Apart from Wnt1, most of the patterning activity of the IsO is conferred by only one molecule, the secreted fibroblast growth factor 8 (*Fgf8*) (Martinez, 2001). The expression of *Wnt1* and *Fgf8* and the positioning of the corresponding domains at the rostral and caudal border of the MHB, respectively, was not changed in the *Fzd6*^{-/-} embryos at E10.5, when this boundary is readily established in the wild-type (Fig. 2A–L). The expression of *Wnt1* and *Fgf8* on consecutive coronal sections of the midbrain and rostral hindbrain was also not changed in the *Fzd6*^{-/-} embryos at E12.5 (Fig. 2M–T and data not shown), indicating that removal of the *Fzd6* receptor does not affect the expression of these two IsO genes over time. As the *Fzd6*^{-/-} mutant embryos did not exhibit any gross morphological and histological deficits in the MHR at E10.5, E12.5, and E17.5 (data not shown), we concluded that the positioning of

the MHB, the activity of the IsO at this boundary, and consequently the patterning of the MHR are not affected by the loss of *Fzd6* receptor function in the mouse embryo. The Wnt1 signal required for these processes is, therefore, likely to be transduced by an alternative or redundant *Fzd* receptor in the *Fzd6*^{-/-} mutants.

Although the establishment of the MHB was not influenced by the loss of *Fzd6*, the prominent expression of this receptor in *Aldh1a1*⁺ mDA precursors within the caudal cephalic flexure might have affected the development of these precursors into mDA neurons. Therefore, we analyzed the different stages of mDA neuron generation in *Fzd6*^{-/-} mutant embryos. In addition to *Aldh1a1*, mDA postmitotic precursors express *Nr4a2* (*Nurr1*), an orphan nuclear receptor required for the activation of the *Th*, vesicular monoamine transporter 2 (*Vmat2/Slc18a2*) and *DA transporter* (*Dat/Slc6a3*) genes (Perlmann and Wallen-Mackenzie, 2004). At E10.5, *Aldh1a1*⁺ mDA progenitors and *Nr4a2*⁺ postmitotic precursors arose normally in the *Fzd6*^{-/-} mutants (see Supp. Fig. S1, which is available online). Differentiation of these precursors into Th⁺, Pitx3⁺ (a homeodomain transcription factor [TF] required for the proper development and survival of a subset of mDA neurons; Smidt et al., 2004) and *Dat*⁺ mDA neurons at E12.5, and the subsequent survival of these neurons until E17.5, were not affected in the *Fzd6*^{-/-} mutants (Fig. 2U–X, Fig. S1). The Pou4f1⁺ (*Brn3a*) domain in the E12.5 midbrain, giving rise to red nucleus (RN) neurons in the VM (Fedtsova and Turner, 1995), and to glutamatergic neurons in the DM (Nakatani et al., 2007), was also not affected in the *Fzd6*^{-/-} mutants (Fig. S1). This suggested that the lack of a neural and in particular mDA phenotype in the *Fzd6*^{-/-} mutants might be due to the redundant function of another *Fzd* receptor.

The Number of Th⁺ mDA Neurons Is Reduced in the *Fzd3*^{-/-} Embryos at E12.5

Fzd3 is expressed throughout the anterior neural tube (Fischer et al.,

2007), and this made it a strong candidate to act redundantly with *Fzd6* in the development of the MHR and of mDA neurons. *Fzd3*^{-/-} mutants do not have gross morphological abnormalities in the MHR except for an open neural tube phenotype at low penetrance (Wang et al., 2002; and data not shown). Even though the generation of *Aldh1a1*⁺ and *Nr4a2*⁺ mDA precursors did not appear to be affected in the *Fzd3*^{-/-} embryos at E10.5 (Fig. S2), the number of Th⁺ mDA neurons was significantly reduced by an average of 42% in the *Fzd3*^{-/-} mutants at E12.5 (Fig. 3A–G). The number of Pitx3⁺ cells was also reduced in the *Fzd3*^{-/-} embryos at this stage, but this reduction did not reach statistical significance (data not shown). The Th⁺ cell numbers appeared to recover at E13.5, and although a slight reduction of Th⁺ mDA neurons was still apparent at E17.5 in the *Fzd3*^{-/-} mutants, this difference was statistically not significant (Fig. 3G). Apart from the reduced mDA neuron numbers, a medio-lateral broadening of the Th⁺, Pitx3⁺, *Nr4a2*⁺, and *Dat*⁺ mDA domain, particularly in the caudal midbrain, was clearly evident in the *Fzd3*^{-/-} mutants at E12.5 and E13.5 (Fig. 3A–F, Fig. S2), but was not detected at later embryonic stages (Fig. S2 and data not shown). The transient reduction in mDA neuron numbers and broadening of the mDA domain in the *Fzd3*^{-/-} mutants did not appear to affect other neuronal populations such as the Pou4f1⁺ RN neurons arising from an adjacent domain in the VM (Fig. 3H,I).

The reduced numbers of Th⁺ mDA neurons in the E12.5 *Fzd3*^{-/-} embryos could have been the consequence of an impaired proliferation of their progenitors or survival of the postmitotic neurons. We, therefore, assessed the number of cells expressing phosphorylated Histone H3 (pH3), a mitotic marker, or cleaved (activated) Caspase3 (cCasp3), an apoptotic marker, in the *Fzd3*^{-/-} VM at E10.5, E12.5, E13.5, or E17.5 (Fig. 3J–M and data not shown). The number of mitotic (pH3⁺) cells was not significantly changed in the *Fzd3*^{-/-} VM at E10.5 or E12.5 (Fig. 3N), the time period during which most mDA neurons are presumably born in the

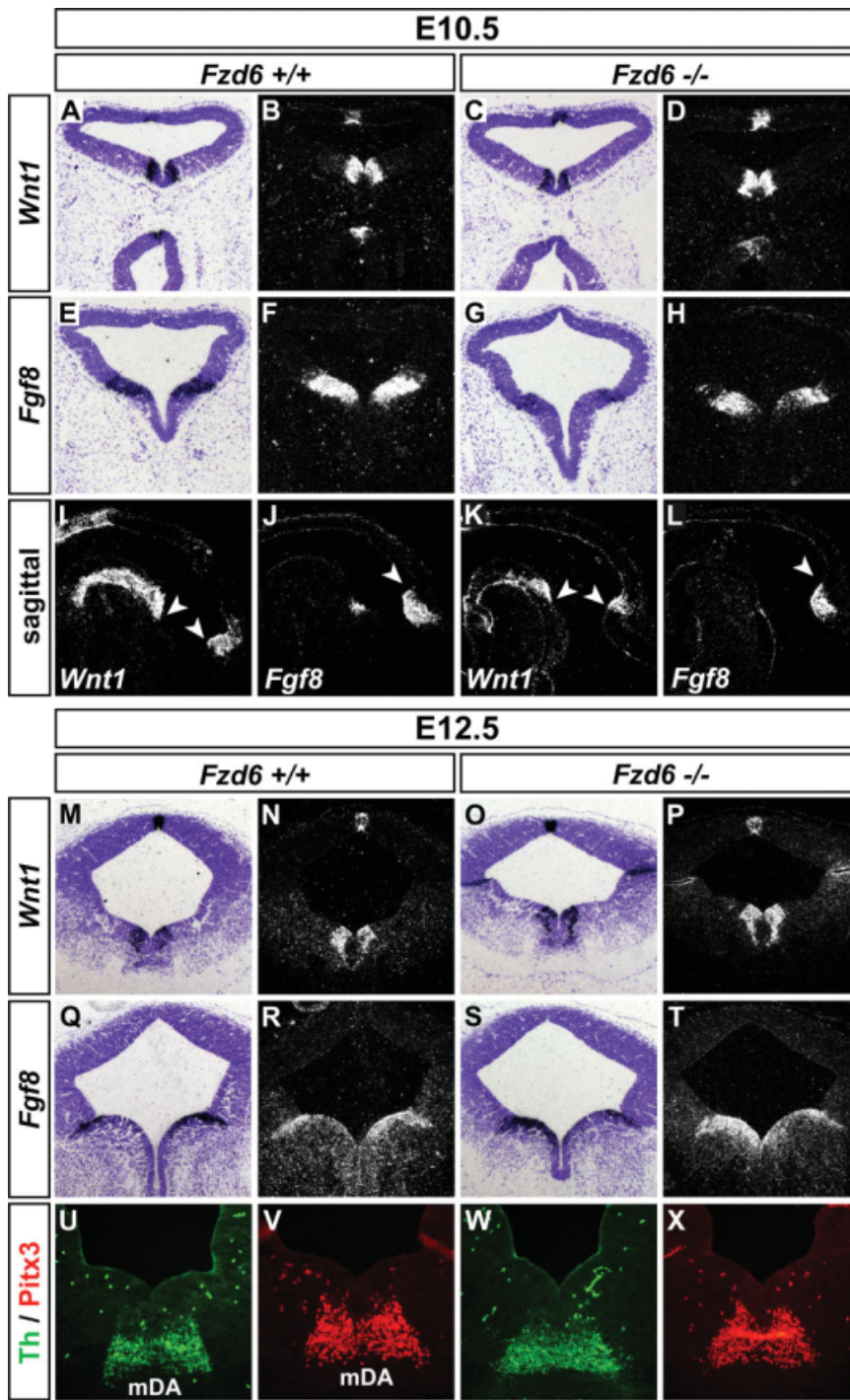


Fig. 2. *Wnt1* and *Fgf8* expression at the MHB and the development of mDA neurons are not affected in *Fzd6*^{-/-} embryos. Representative coronal (A–H, M–X) and midsagittal (I–L) sections from E10.5 (A–L) and E12.5 (M–X) *Fzd6*^{+/+} (A,B,E,F,I,J,M,N,Q,R,U,V) and *Fzd6*^{-/-} (C,D,G,H,K,L,O,P,S,T,W,X) mouse embryos hybridized with riboprobes for *Wnt1* (A–D,I,K,M–P) and *Fgf8* (E–H,J,L,Q–T), or immunostained with antibodies for Th (green, U,W) and Pitx3 (red, V,X). Dorsal is at the top, anterior to the left. Arrowheads in I–L point at the caudal (I,K) or rostral (J,L) expression boundaries of the corresponding genes demarcating the position of the MHB. The section shown in J was cut at a more lateral level than the section shown in L; the ventral *Fgf8* domain in the BP (sparing the FP) is thus visible in the section shown in J.

mouse embryo. Moreover, only very few if any apoptotic (cCasp3⁺) cells were detected in the *Fzd3*^{-/-} VM at

E12.5, E13.5, and E17.5, similar to the wild-type (data not shown). We thus concluded that the loss of the

Fzd3 receptor in the VM in general and in mDA precursors in particular has no influence on the proliferation and survival of these cells, but appears to affect the differentiation of mDA precursors into Th⁺ mDA neurons.

Fzd3^{-/-}; *Fzd6*^{-/-} Double Mutant Mouse Embryos Have a Severe Midbrain Morphogenesis Defect

The lack of an overall MHB phenotype in the *Fzd6*^{-/-} and *Fzd3*^{-/-} single mutants, and the transient mDA phenotype in the *Fzd3*^{-/-} embryos, suggested a redundant function of the two receptors in these processes. We, therefore, proceeded with the analysis of *Fzd3*^{-/-}; *Fzd6*^{-/-} double mutants. Due to the low frequency of double mutant embryos derived from our breeding scheme, we focused our analyses on embryonic stages E10.5 (when the IsO is already established at the MHB) and E12.5 (when different neuronal populations are emerging in the midbrain). Five out of seven (71%) double mutant *Fzd3*^{-/-}; *Fzd6*^{-/-} and two *Fzd3*^{-/-}; *Fzd6*^{+/-} embryos dissected at E12.5, as well as two out of three (67%) double mutant *Fzd3*^{-/-}; *Fzd6*^{-/-} embryos dissected at E10.5, had the outer appearance of an open neural tube (Fig. 4A,B). Furthermore, all *Fzd3*^{-/-}; *Fzd6*^{-/-} and *Fzd3*^{-/-}; *Fzd6*^{+/-} mutants dissected at E10.5 and E12.5 had a curly tail (Fig. 4A,B), similar to what was reported by Wang et al. (2006a). Upon closer inspection of these embryos, however, we noted that their anterior neural tube was closed and in some cases it exhibited several bulges along the antero-posterior (A/P) axis (Fig. 4A,B). Nissl-stained coronal sections at the level of the forebrain, midbrain, and hindbrain, indeed, confirmed that the anterior neural tube of these mutants was completely closed and covered by mesenchyme (Fig. 4D–I). These sections also revealed a massive growth of dorsal neural tissue into the mesencephalic (third) ventricle in three out of seven (43%) double mutant *Fzd3*^{-/-}; *Fzd6*^{-/-} embryos dissected at E12.5 (Fig. 4D,E). In fact, the third ventricle was almost entirely occluded by the protruding neural tissue, which had also fused in part

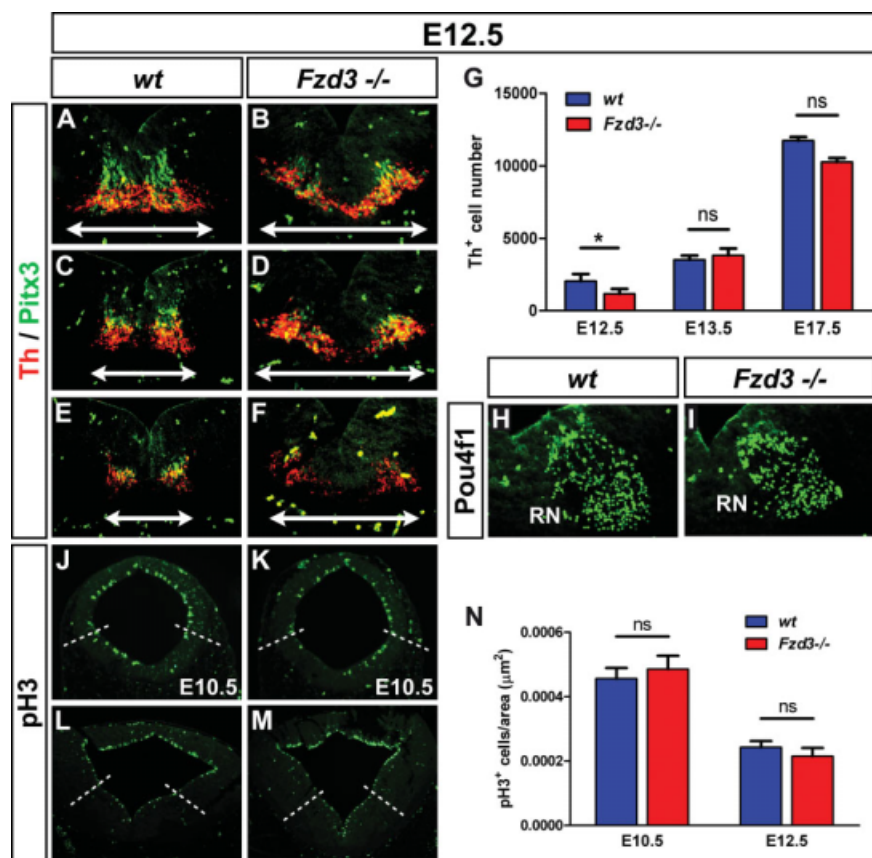


Fig. 3. The number of Th⁺ mDA neurons is significantly reduced in *Fzd3*^{-/-} embryos at E12.5. **A–F, H–M:** Representative coronal midbrain sections from E12.5 (A–F, H, I, L, M) and E10.5 (J, K) wild-type (*wt* [*Fzd3*^{+/+} or *Fzd3*^{+/-}]; A, C, E, H, J, L) and *Fzd3*^{-/-} (B, D, F, I, K, M) mouse embryos immunostained with antibodies for Th (red, A–F), Pitx3 (green, A–F), Pou4f1 (Brn3a; H, I), and phospho-Histone H3 (pH3; J–M). Dorsal is at the top. Sections in A–F were taken at successive anterior (A, B) to posterior (E, F) levels of the midbrain. Double arrows in A–F depict the broadening of the mDA domain in *Fzd3*^{-/-} embryos, in particular in the caudal midbrain. Pou4f1⁺ red nucleus (RN) neurons are not affected in the *Fzd3*^{-/-} mutants (H, I). White broken lines in J–M indicate the approximate dorsal limit of the VM area used for quantification of pH3⁺ cells. **G:** Quantification of the number of Th⁺ mDA neurons in *wt* and *Fzd3*^{-/-} embryos at E12.5, E13.5, and E17.5 (significant interaction effect in the two-way ANOVA, $P = 0.025$). (E12.5: *wt*, 2,040 ± 494; *Fzd3*^{-/-}, 1,169 ± 340 mean ± s.e.m.; * $P = 0.031$ in the paired *t*-test; $n = 3$ pairs of mice; E13.5: *wt*, 3,524 ± 282; *Fzd3*^{-/-}, 3,816 ± 473 mean ± s.e.m.; ns, not significant, $P = 0.425$; $n = 3$ pairs of mice; E17.5: *wt*, 1,1730 ± 255; *Fzd3*^{-/-}, 10,252 ± 277 mean ± s.e.m.; ns, not significant, $P = 0.159$; $n = 2$ pairs of mice). **N:** Quantification of mitotic (pH3⁺) cells/ μm^2 in the *wt* and *Fzd3*^{-/-} VM at E10.5 and E12.5 (E10.5: *wt*, 0.000456 ± 0.0000330x; *Fzd3*^{-/-}, 0.000486 ± 0.0000418 mean ± s.e.m.; ns, not significant, $P = 0.774$ in the one-way ANOVA for repeated measurements; $n = 3$ mice in each group with 7–8 sections each; E12.5: *wt*, 0.000243 ± 0.0000195; *Fzd3*^{-/-}, 0.000215 ± 0.0000253 mean ± s.e.m.; ns, not significant, $P = 0.425$; $n = 2$ pairs of mice with 7–8 sections each).

with VM neuroepithelium (Fig. 4D,E). All other *Fzd3*^{-/-}; *Fzd6*^{-/-} double mutants analyzed at E10.5 or E12.5 did not display this massive protrusion of dorsal neural tissue, but showed a collapse of the brain ventricles and an apparently thickening of the neuroepithelium and of the mesenchymal layer surrounding it, particularly in the dorsal MHR (Fig. 4F–I). Moreover, the *Fzd3*^{-/-}; *Fzd6*^{-/-} double mutant midbrain was broadened laterally and

tended to be shortened along the D/V axis at E12.5 (Fig. 4C). Altogether, the simultaneous loss of *Fzd3* and *Fzd6* leads to a severe midbrain morphogenesis defect that is not an open (exencephalic) anterior neural tube. Since such a neurulation phenotype has to the best of our knowledge not been described before, we tried to characterize in more detail the midbrain defect in the *Fzd3*^{-/-}; *Fzd6*^{-/-} double mutants.

Cell Proliferation Is Not Increased in the *Fzd3*^{-/-}; *Fzd6*^{-/-} Double Mutant Midbrain at E10.5

The collapse of the brain ventricles and apparently thickening of the neuroepithelium in the MHR of the *Fzd3*^{-/-}; *Fzd6*^{-/-} embryos already at E10.5, which in its most extreme case might lead to the massive protrusion of dorsal neural tissue and occlusion of the third ventricle at E12.5, suggested an increased cell proliferation in the double mutant midbrain. Wnts are known to regulate cell proliferation and in particular the transition between G1 to S phase of the cell cycle (Megason and McMahon, 2002). We therefore analyzed the distribution and number of BrdU-labeled cells in the midbrain neuroepithelium of wild-type and *Fzd3*^{-/-}; *Fzd6*^{-/-} embryos at E10.5. The distribution of BrdU⁺ cells was similar in wild-type and double mutant embryos at this stage (Fig. 5A–F, H). For the quantification of BrdU⁺ cells, we had to account for the fact that even in the wild-type embryo, cell proliferation is higher in the DM compared to the VM (Fig. 5G). We thus defined the border between the DM and VM areas in wild-type and double mutant embryos roughly at the position of the dorsolateral hinge-points, as depicted in Figure 5A, B. Although the total number of BrdU⁺ cells in the DM and VM tended to be increased in the *Fzd3*^{-/-}; *Fzd6*^{-/-} double mutants, this increase did not reach statistical significance (data not shown). We obtained a similar result when we calculated the density of the BrdU-labeled cells in the DM and VM of wild-type and *Fzd3*^{-/-}; *Fzd6*^{-/-} embryos (Fig. 5G), indicating that cell proliferation, and in particular cells in the S phase of the cell cycle, are not significantly increased in the double mutant midbrain at E10.5.

The nuclear staining of proliferating BrdU⁺ cells located at the ventricular surface of the neuroepithelium, however, revealed another defect in the double mutants. The basal membrane at the ventricular surface of the neuroepithelium appeared to be focally disrupted by filopodia-like

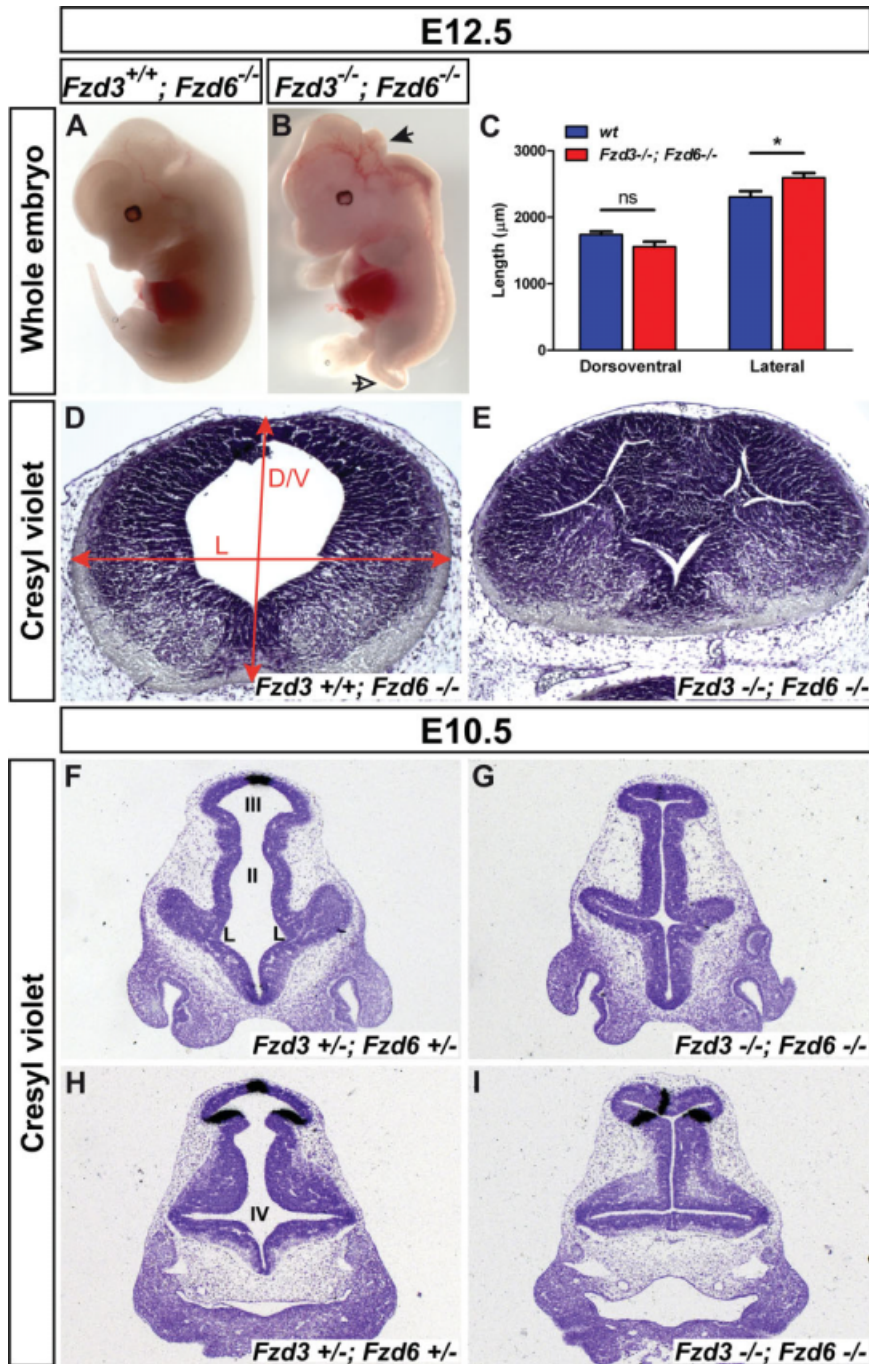


Fig. 4. A severe midbrain morphogenesis defect is already evident at E10.5 in *Fzd3^{-/-}; Fzd6^{-/-}* double mutant embryos. **A,B:** Lateral views of an *Fzd3^{+/+}; Fzd6^{-/-}* “wild-type” (**A**) and an *Fzd3^{-/-}; Fzd6^{-/-}* double mutant (**B**) embryo at E12.5. Black arrow in **B** points at the mid-/hindbrain “bulge” in the double mutant embryo. Note a similar bulge from the caudal forebrain/midbrain in this embryo. Open arrow in **B** points at the curly tail of the double mutant. **C:** Quantification of the dorsoventral (D/V) and left-right (lateral, L) extent of the midbrain in E12.5 wild-type (wt) and *Fzd3^{-/-}; Fzd6^{-/-}* double mutant embryos, as depicted by red double arrows in **D**. Significant interaction effect in the two-way ANOVA, $P = 0.002$. (D/V: wt, $1741.4 \pm 46.6 \mu\text{m}$; *Fzd3^{-/-}; Fzd6^{-/-}*, $1,559.6 \pm 75.0 \mu\text{m}$ mean \pm s.e.m.; ns, not significant, $P = 0.053$ in the one-way ANOVA for repeated measurements; L: wt, $2305.6 \pm 88.9 \mu\text{m}$; *Fzd3^{-/-}; Fzd6^{-/-}*, $2,596.5 \pm 68.9 \mu\text{m}$ mean \pm s.e.m.; * $P = 0.018$; $n = 3$ pairs of embryos with 4 sections each). **D–I:** Representative Nissl-stained coronal sections at midbrain (**D,E**), forebrain (**F,G**), and anterior hindbrain (**H,I**) levels from *Fzd3^{+/+}; Fzd6^{-/-}* or *Fzd3^{+/-}; Fzd6^{+/-}* “wild-type” (**D,F,H**) and *Fzd3^{-/-}; Fzd6^{-/-}* double mutant (**E,G,I**) embryos at E12.5 (**D,E**) and E10.5 (**F–I**). Dorsal is at the top. Black staining in **F–I** are radioactive in situ hybridization signals for *Wnt1*. L, II, III, IV: lateral (telencephalic), second (diencephalic), third (mesencephalic), and fourth (metencephalic) brain ventricles, respectively.

cellular protrusions and BrdU⁺ cell nuclei extending into the remaining ventricular cavity of the double mutant midbrain (Fig. 5D,H). These focal disruptions occurred more often in the DM than in the VM, and were never observed in the wild-type midbrain (Fig. 5C–F,H). We thus propose that these focal disruptions of the basal membrane and cellular protrusions might be the sites at which a later “fusion” of dorsal and ventral neural tissues occurs, especially if they face each other on both sides of the remaining ventricular cavity, as depicted in Figure 5D.

D/V Patterning Is Not Affected in the *Fzd3^{-/-}; Fzd6^{-/-}* Double Mutant Midbrain

We next assessed whether the midbrain morphogenesis defect in the *Fzd3^{-/-}; Fzd6^{-/-}* embryos might be due to a defective D/V patterning. The dorsal (roof plate, RP) and ventral (FP) midline of the midbrain is characterized by the expression of *Wnt1* (Wilkinson et al., 1987), *Lmx1a* (Millonig et al., 2000; Chizhikov and

Fig. 6. D/V patterning is not affected in the *Fzd3^{-/-}; Fzd6^{-/-}* double mutant midbrain at E12.5. **A–N:** Representative coronal midbrain sections from E12.5 “wild-type” (wt) (*Fzd3^{+/+}; Fzd6^{-/-}* or *Fzd3^{+/-}; Fzd6^{+/-}*; **A,C,E,G,H,K,L**) and *Fzd3^{-/-}; Fzd6^{-/-}* double mutant (**B,D,F,I,J,M,N**) embryos hybridized with riboprobes for *Wnt1* (**A,B**), *Lmx1a* (**C,D**), and *Lmx1b* (**E,F**), or immunostained with antibodies for Dbx1 (red) and Nkx2-2 (green) (**G–J**), or Nkx6-2 (red) and Pax7 (green) (**K–N**). Dorsal is at the top. The section in **B** was taken at a more anterior level than the section in **A**. Red broken lines in **A** and **C** delimit the roof plate (RP) and the floor plate (FP), respectively. Black and white arrows in **B,D,F** point at the stripe of *Wnt1⁺*, *Lmx1a⁺*, and *Lmx1b⁺* cells extending from the dorsal surface ventrally across the protruding dorsal neural tissue. **H,J,L,N** are higher magnifications of the right half of the midbrain shown in **G,I,K,M**, respectively. **O–R:** Representative coronal midbrain sections from *Fzd3^{+/+}; Fzd6^{-/-}* “wild-type” (wt; **O,P**) and *Fzd3^{-/-}; Fzd6^{-/-}* (**Q,R**) embryos pulse-labeled with BrdU for 2 hr at E12.5. Dorsal is at the top. **P** and **R** are higher magnifications of **O** and **Q**, respectively. Black broken lines in **O,Q** indicate the approximate position of the border between the DM and VM areas used for the quantification of pH3⁺ and BrdU⁺ cells in E12.5 embryos. Quantification of BrdU⁺ cells/ μm^2 in these embryos is shown in Figure 7N.

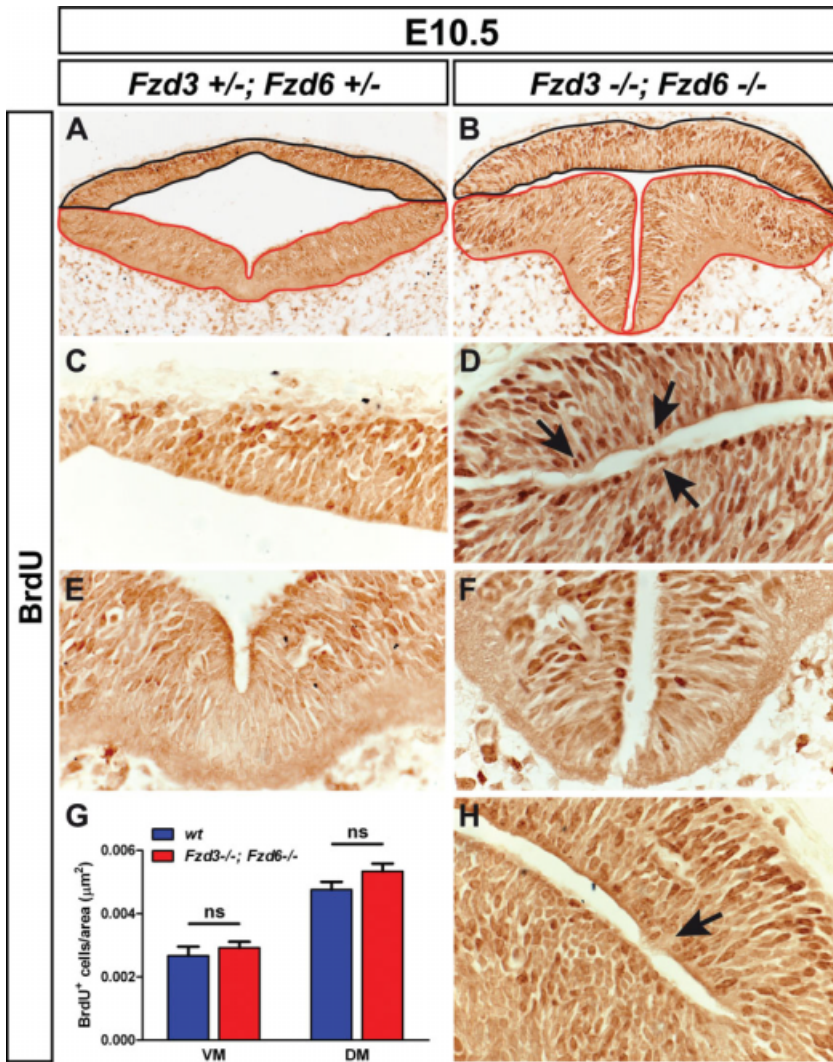


Fig. 5.

Millen, 2004b), and *Lmx1b* (Chizhikov and Millen, 2004a). At E10.5, *Wnt1* and *Lmx1a* were expressed in a perpendicular stripe of cells across the thickened dorsal neuroepithelium, at a position that might correspond to the RP of the double mutant midbrain (Fig. S3). A similar pattern of *Wnt1* and *Lmx1a* expression as in the FP of the wild-type embryo was observed in the *Fzd3*^{-/-}; *Fzd6*^{-/-}

Fig. 5. Cell proliferation is not significantly increased but cellular protrusions are evident at E10.5 in the neuroepithelium of *Fzd3*^{-/-}; *Fzd6*^{-/-} double mutant embryos. A-F, H: Representative coronal midbrain sections from *Fzd3*^{+/-}; *Fzd6*^{+/-} “wild-type” (wt; A,C,E) and *Fzd3*^{-/-}; *Fzd6*^{-/-} double mutant (B,D,F,H) embryos pulse-labeled with BrdU for 2 hr at E10.5. Dorsal is at the top. C,E and D,F are higher magnifications of the DM (C,D) and VM (E,F) shown in A and B, respectively. Black arrows in D,H point at the sites where the basal lamina at the ventricular surface of the neuroepithelium appeared to be disrupted by filopodia-like cellular protrusions and cell nuclei extending into the ventricular cavity of the double mutant midbrain. G: Quantification of BrdU⁺ cells/μm² in the VM (area delineated with a red line in A,B) and DM (area delineated with a black line in A,B) of wt and *Fzd3*^{-/-}; *Fzd6*^{-/-} double mutant embryos at E10.5 (VM: wt, 0.00267 ± 0.00028; *Fzd3*^{-/-} *Fzd6*^{-/-}, 0.00292 ± 0.00019 mean ± s.e.m.; DM: wt, 0.00476 ± 0.00025; *Fzd3*^{-/-} *Fzd6*^{-/-}, 0.00534 ± 0.00024 mean ± s.e.m; Genotype effect in two-way ANOVA without interaction not significant (ns), P = 0.096, post-hoc tests not appropriate; n = 2 pairs of embryos with 4 sections each).

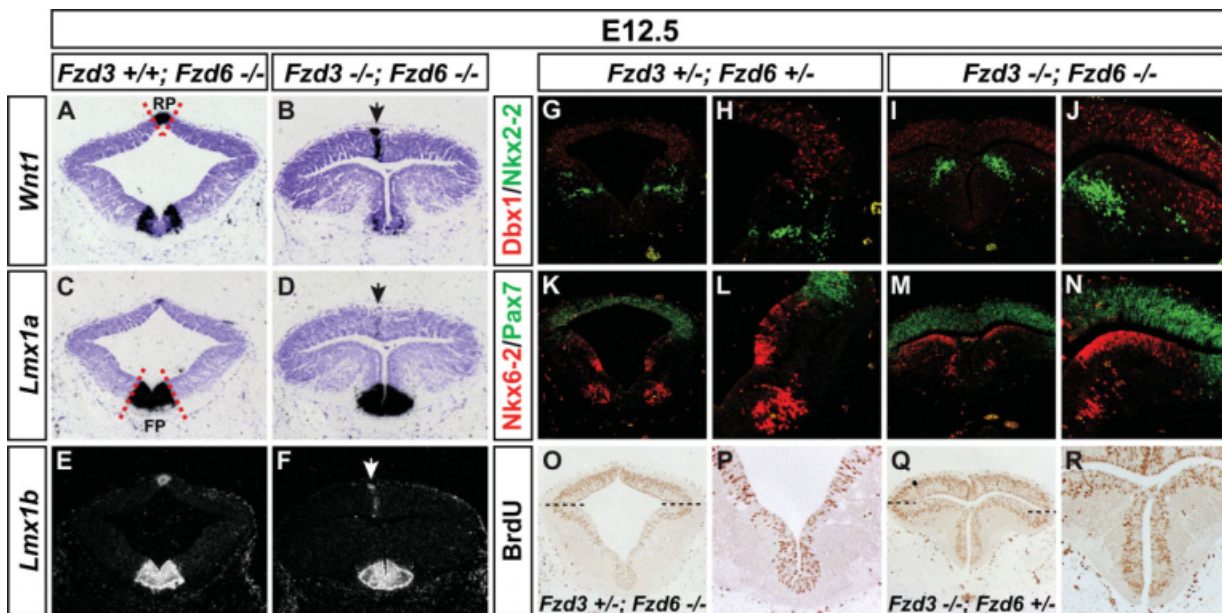


Fig. 6.

double mutant VM at E10.5, except for a slightly aberrant morphology and broadening of their expression domains due to the thickened and protruding ventral neural tissue in the double mutants (Fig. S3). Moreover, the A/P extent of the *Wnt1*⁺ and *Lmx1a*⁺ domains did not appear to be affected in the double mutants at E10.5, as assessed on consecutive coronal sections of the wild-type and double mutant midbrain (Fig. S3). The alar plate (AP) is the DM domain adjacent to the RP and characterized by the expression of *Dbx1* and *Pax7*, the BP is the VM domain adjacent to the FP and characterized by the expression of *Nkx6-1* and *Nkx6-2*, and an intermediate zone located at the ventrolateral sulcus of the midbrain is characterized by the expression of *Nkx2-2* (Prakash et al., 2009). The spatial relationship of the *Dbx1*⁺ and *Pax7*⁺ domains dorsally, and of the *Nkx2-2*⁺ and *Nkx6-2*⁺ domains ventrally, was preserved in the *Fzd3*^{-/-}; *Fzd6*^{-/-} embryos at E10.5, despite the altered morphology of the double mutant midbrain (Fig. S3).

The D/V positioning and A/P extent of the *Wnt1*⁺, *Lmx1a*⁺, *Lmx1b*⁺, *Dbx1*⁺, *Nkx2-2*⁺, *Pax7*⁺ and *Nkx6-2*⁺ domains were still preserved in the *Fzd3*^{-/-}; *Fzd6*^{-/-} double mutant midbrain at E12.5 (Fig. 6A–N and data not shown). At this stage, the ventral boundary of the dorsal *Dbx1*⁺ domain abuts the *Nkx2-2*⁺ domain in the mantle zone (MZ) of the lateral midbrain, and the ventral boundary of the dorsal *Pax7*⁺ domain abuts the dorsal *Nkx6-2*⁺ domain in the ventricular (VZ)/subventricular (SVZ) zone of the lateral midbrain (Fig. 6G,H,K,L). These D/V boundaries of expression were not altered in the double mutants, indicating that D/V positional information is conserved in the *Fzd3*^{-/-}; *Fzd6*^{-/-} midbrain despite the severe morphogenesis defect.

A Reduction of *Fzd6* Gene Dosage on an *Fzd3*^{-/-} Background Is Sufficient to Cause the Severe Midbrain Morphogenesis Defect

In the absence of an obvious D/V patterning defect in the *Fzd3*^{-/-}; *Fzd6*^{-/-} embryos, we then asked whether

the number of proliferating cells, and in particular S phase cells, was increased in the double mutant midbrain at E12.5, thereby leading to the massive growth of dorsal neural tissue and occlusion of the third ventricle observed in three out of seven (43%) double mutant embryos at this stage. Due to the low frequency of double mutants expected from our breeding scheme, we did not obtain BrdU pulse-labeled *Fzd3*^{-/-}; *Fzd6*^{-/-} embryos at E12.5. However, we noted that embryos genotyped as *Fzd3*^{-/-}; *Fzd6*^{+/-} also had the outer appearance of an open neural tube at this stage, and we therefore proceeded with the analysis of these embryos. We used their *Fzd3*^{+/-}; *Fzd6*^{-/-} littermates for comparison and for the assessment of a gene dosage effect. Coronal sections through the anterior

neural tube revealed a brain morphogenesis defect in the *Fzd3*^{-/-}; *Fzd6*^{+/-} but not in the *Fzd3*^{+/-}; *Fzd6*^{-/-} embryos that was indistinguishable from the defect in two out of seven (29%) and two out of three (67%) *Fzd3*^{-/-}; *Fzd6*^{-/-} double mutants analyzed at E12.5 and E10.5, respectively (data not shown). At E12.5, the *Fzd3*^{-/-}; *Fzd6*^{+/-} embryos showed a similar collapse of the third ventricle and thickening of the midbrain neuroepithelium as the *Fzd3*^{-/-}; *Fzd6*^{-/-} double mutants (Fig. 6O–R), and we therefore assessed the number and distribution of BrdU-labeled cells in their midbrain. Even though the total number of BrdU⁺ cells was significantly ($P < 0.001$) increased in the VM but not in the DM of the *Fzd3*^{-/-}; *Fzd6*^{+/-} embryos (data not shown), their density was not significantly

Fig. 7. Cell proliferation is significantly increased at E12.5 in the VM and DM of *Fzd3*^{-/-}; *Fzd6*^{-/-} embryos with protrusion of dorsal neural tissue. **A–L:** Representative coronal midbrain sections from E12.5 *Fzd3*^{+/-}; *Fzd6*^{-/-} “wild-type” (A,C,E,G,I,K) and *Fzd3*^{-/-}; *Fzd6*^{-/-} double mutant (B,D,F,H,J,L) embryos immunostained with antibodies for phospho-Histone H3 (pH3; A,B), cyclin D1 (Ccnd1; C,D), p27^{Kip1} (Cdkn1b; E,F), Sox2 (G,H), Mash1 (Ascl1; I,J), and NeuN (K,L). Dorsal is at the top. Double mutant embryos in B,F,H,J,L show already a massive protrusion of dorsal neural tissue into the third ventricle, whereas dorsal neural tissue is beginning to protrude in the embryo shown in D. White arrow in F points at the stripe of Cdkn1b⁺ cells extending from the dorsal surface ventrally across the protruding dorsal neural tissue. **M:** Quantification of mitotic (pH3⁺) cells/ μm^2 in the VM and DM (delimitation of areas as in Fig. 6) of *wt* and *Fzd3*^{-/-}; *Fzd6*^{-/-} embryos with protruding dorsal neural tissue at E12.5. Significant genotype and region effect in the one-way ANOVA without interaction, both $P < 0.0001$. (Post-hoc genotype comparisons with P value adjustment: VM: *wt*, 0.000211 ± 0.0000134 ; *Fzd3*^{-/-}; *Fzd6*^{-/-}, 0.000323 ± 0.0000191 mean \pm s.e.m.; $***P = 0.0006$ in the one-way ANOVA for repeated measurements; DM: *wt*, 0.000573 ± 0.0000201 ; *Fzd3*^{-/-}; *Fzd6*^{-/-}, 0.000687 ± 0.0000337 mean \pm s.e.m.; $***P < 0.0001$; $n = 3$ pairs of embryos with 11–16 sections each). **N:** Quantification of BrdU⁺ cells/ μm^2 in the VM and DM of *wt* and *Fzd3*^{-/-}; *Fzd6*^{+/-} embryos without protruding dorsal neural tissue at E12.5. Significant interaction effect in the two-way ANOVA, $P = 0.009$. (Region-specific genotype comparisons: VM: *wt*, 0.00135 ± 0.0000965 ; *Fzd3*^{-/-}; *Fzd6*^{+/-}, 0.00344 ± 0.000439 mean \pm s.e.m.; ns, not significant, $P = 0.053$ in the one-way ANOVA for repeated measurements; DM: *wt*, 0.00506 ± 0.000182 ; *Fzd3*^{-/-}; *Fzd6*^{+/-}, 0.00516 ± 0.000526 mean \pm s.e.m.; ns, not significant, $P = 0.928$; $n = 2$ pairs of embryos with 5 sections each).

Fig. 8. Th⁺ and Pitx3⁺ mDA and Pou4f1⁺ RN neurons are specified correctly in the *Fzd3*^{-/-}; *Fzd6*^{-/-} double mutant embryos at E12.5. **A–F,I,J:** Representative coronal midbrain sections from E12.5 *Fzd3*^{+/-}; *Fzd6*^{+/-} and *Fzd3*^{+/-}; *Fzd6*^{-/-} “wild-type” (*wt*; A,C,E,I) and *Fzd3*^{-/-}; *Fzd6*^{-/-} double mutant (B,D,F,J) embryos immunostained with antibodies for Th (red, A–F), Pitx3 (green, A–F), and Pou4f1 (Brn3a; I,J). Dorsal is at the top. Sections in A–F were taken at successive anterior (A,B) to posterior (E,F) levels of the midbrain. Double arrows in E,F depict the broadening of the mDA domain in the *Fzd3*^{-/-}; *Fzd6*^{-/-} caudal midbrain. White arrows in J point at the cellular defects within the Pou4f1⁺ RN domain. **G:** Quantification of the number of Th⁺ mDA neurons in *wt* and *Fzd3*^{-/-}; *Fzd6*^{-/-} double mutant embryos at E11.5 and E12.5 (E11.5: *wt*, 438 ± 177 ; *Fzd3*^{-/-}; *Fzd6*^{-/-}, 349 ± 18 mean \pm s.e.m.; $n = 2$ pairs of mice; E12.5: *wt*, $2,080 \pm 847$; *Fzd3*^{-/-}; *Fzd6*^{-/-}, $1,537 \pm 536$ mean \pm s.e.m.; $n = 4$ pairs of mice; genotype effect in two-way ANOVA without interaction not significant (ns), $P = 0.181$, post-hoc tests not appropriate). **H:** Quantification of the density of Th⁺ cells/ μm^2 in *wt* and *Fzd3*^{-/-}; *Fzd6*^{-/-} double mutant embryos at E11.5 and E12.5. Significant genotype effect in the one-way ANOVA without interaction, $P < 0.004$. (Post-hoc genotype comparisons with P value adjustment: E11.5: *wt*, 0.00183 ± 0.000292 ; *Fzd3*^{-/-}; *Fzd6*^{-/-}, 0.00124 ± 0.0000606 mean \pm s.e.m.; ns, not significant, $P = 0.593$ in the paired t -test; $n = 2$ pairs of mice; E12.5: *wt*, 0.00286 ± 0.000303 ; *Fzd3*^{-/-}; *Fzd6*^{-/-}, 0.00184 ± 0.000186 mean \pm s.e.m.; $*P = 0.0021$; $n = 4$ pairs of mice).

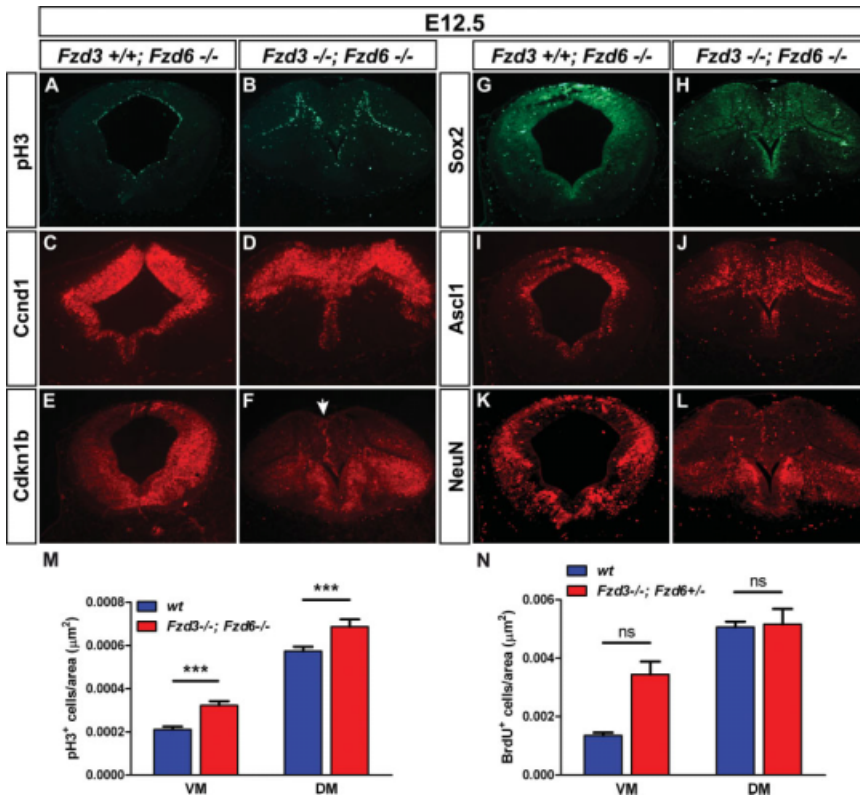


Fig. 7.

increased in these embryos (Fig. 7N). Two conclusions were drawn from these experiments: firstly, the reduction of *Fzd6* gene dosage on an *Fzd3* null background is sufficient to cause the severe midbrain morphogenesis defect, but not vice versa. Secondly, the tendency towards an increased number of proliferating S phase cells in the VM of the *Fzd3*^{-/-}; *Fzd6*^{+/-} embryos at E12.5 might be the first sign of an increased proliferation in these mutants, and might contribute to the protrusion of dorsal and ventral neural tissues and to the rescue of mDA neuron numbers in the double mutants (see below).

Increased Cell Proliferation and Delayed Cell Cycle Exit Might Be the Cause for the Massive Growth of Dorsal Neural Tissue in Some *Fzd3*^{-/-}; *Fzd6*^{-/-} Embryos at E12.5

Because of the previous findings, we next investigated whether the massive protrusion of dorsal neural tissue

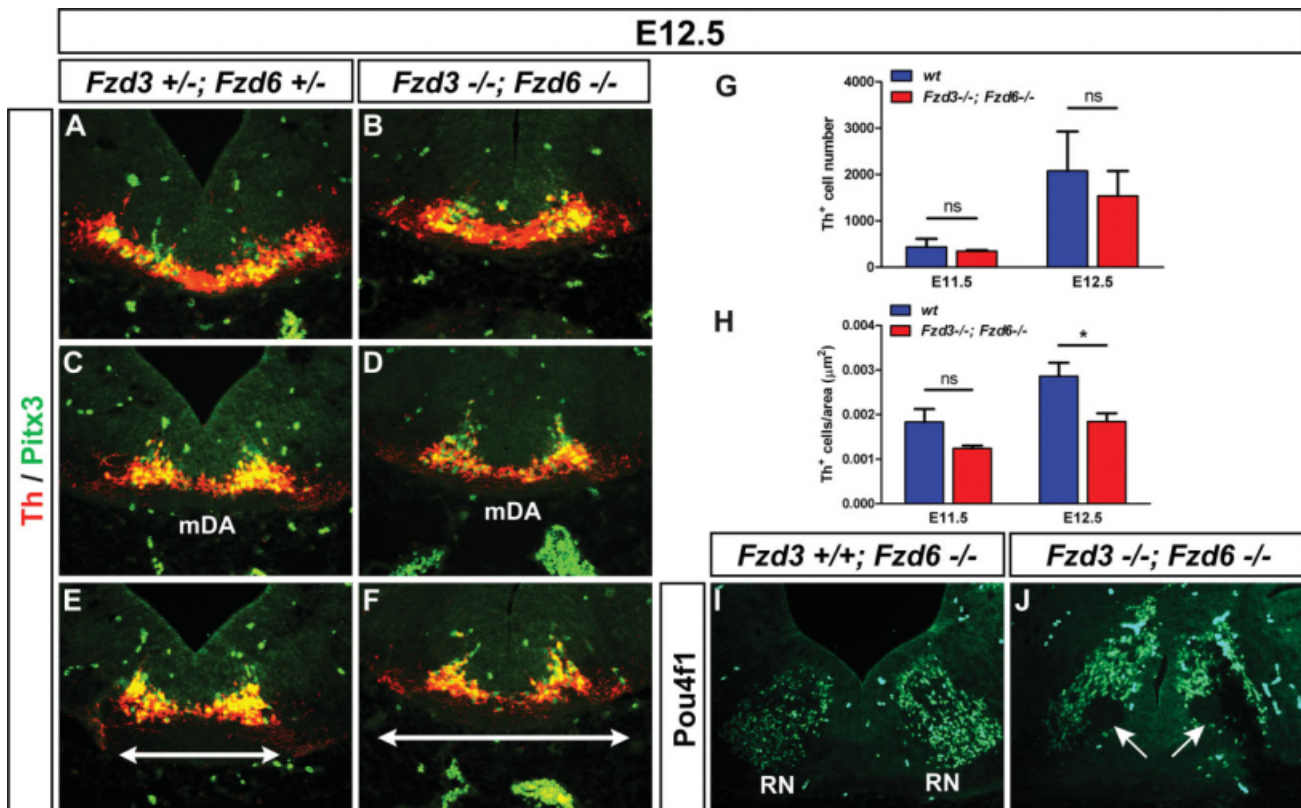


Fig. 8.

in three out of seven (43%) *Fzd3*^{-/-}; *Fzd6*^{-/-} double mutant embryos dissected at E12.5 might be due to the excessive proliferation of dorsal neuroepithelial cells in their midbrain. Although mitotic (pH3⁺) progenitors were mostly confined to the VZ/SVZ lining the occluded third ventricle and pH3⁺ cells were not found inside the protruding tissue mass (Fig. 7A,B), their cell density was significantly increased in the VM and DM of these double mutants (Fig. 7M). Moreover, the protruding dorsal neural tissue contained mostly cells expressing cyclin D1 (*Ccnd1*, a marker for cells in the cell cycle) and only very few cells expressing the cyclin-dependent kinase inhibitor p27^{Kip1} (*Cdkn1b*, a marker for cells exiting the cell cycle) (Fig. 7C–F), suggesting that cell cycle exit was also delayed in the protruding dorsal neural tissue of the double mutants. In line with this finding, the TFs Sox2 and Mash1 (*Ascl1*), markers for proliferating neural progenitors in the midbrain (Kele et al., 2006), were widely expressed across the protruding dorsal neural tissue (Fig. 7G–J), whereas expression of NeuN (*Neuna60*), a marker for postmitotic neurons, was mostly confined to the outer margin (MZ) of the DM and hardly detected within the protruding tissue (Fig. 7K,L). The number of apoptotic (cCasp3⁺) cells, by contrast, was not increased in the double mutant midbrain (data not shown). We therefore concluded that the massive growth of neural tissue in some double mutant embryos at E12.5, leading to the occlusion of the third ventricle, was most likely a consequence of the increased proliferation and delayed cell cycle exit of neural progenitors at this later stage.

Th⁺ and Pitx3⁺ mDA Neurons Are Correctly Specified in the *Fzd3*^{-/-}; *Fzd6*^{-/-} Double Mutants

Finally, we wanted to know if the further reduction of *Fzd* gene dosage and the midbrain morphogenesis defect in the *Fzd3*^{-/-}; *Fzd6*^{-/-} double mutants might have affected the normal development of the mDA and other mid-

brain neuronal populations. Th⁺ and Pitx3⁺ mDA neurons were detected in the *Fzd3*^{-/-}; *Fzd6*^{-/-} VM at E11.5 and E12.5, and although their numbers tended to be reduced in the double mutants, this reduction did not reach statistical significance (Fig. 8A–G and data not shown). However, the Th⁺ cell density was significantly reduced and a medio-lateral broadening of the mDA domain, similar to the *Fzd3*^{-/-} single mutants, was detected in the caudal midbrain of the double mutants at E12.5 (Fig. 8E,F,H). *Wnt1*, *Lmx1a*, and *Lmx1b* are expressed in proliferating mDA progenitors/postmitotic precursors in the midbrain FP and required for the generation of mDA neurons (Smidt et al., 2000; Zervas et al., 2004; Andersson et al., 2006; Prakash et al., 2006; Ono et al., 2007). The expression of these factors in the *Fzd3*^{-/-}; *Fzd6*^{-/-} embryos (Fig. 6A–F, Fig. S3) also indicated the correct specification of mDA precursors in the double mutant VM. Pou4f1⁺ RN neurons emerged from the double mutant VM, but the appearance of this domain was more affected in the *Fzd3*^{-/-}; *Fzd6*^{-/-} embryos (Fig. 8I,J). The Pou4f1⁺ RN domain was elongated along the D/V axis and exhibited a cellular defect in its ventral part (Fig. 8I,J) that might be due to the massive up-folding of ventral neural tissue in the double mutants.

Based on these results, we concluded that the loss of *Fzd6* expression in an *Fzd3*^{-/-} background does not affect the specification of mDA and RN neurons. However, their density and distribution was altered in the double mutant VM, most likely because of the midbrain morphogenesis defect. We also concluded that the transient reduction of Th⁺ mDA neuron numbers, observed in the *Fzd3*^{-/-} single mutants at E12.5, might be compensated in the *Fzd3*^{-/-}; *Fzd6*^{-/-} embryos by the increased proliferation detected in the double mutant VM at this stage.

DISCUSSION

Here we investigated the potential function of the two Fzd receptors,

Fzd3 and *Fzd6*, in midbrain development, based on their prominent expression in this brain region of the midgestational mouse embryo and on the known requirement of Wnt/β-catenin signaling for this process. Our results indicate that the establishment and maintenance of the IsO at the MHB, and the patterning of the midbrain along the D/V axis are not affected in the *Fzd6*^{-/-} and *Fzd3*^{-/-} single, and *Fzd3*^{-/-}; *Fzd6*^{-/-} double mutant embryos. The mDA neurons developed normally in the *Fzd6*^{-/-} embryos, but their number was transiently reduced in the *Fzd3*^{-/-} single mutants at E12.5 and recovered at later stages. This mDA phenotype was rescued in the *Fzd3*^{-/-}; *Fzd6*^{-/-} embryos, probably due to the increased proliferation detected in the double mutant VM at this stage. We, therefore, concluded that *Fzd3* and *Fzd6* are not necessary for the A/P and D/V patterning of the midbrain, and that *Fzd3* but not *Fzd6* plays a role in mDA neuron differentiation. The *Fzd3*^{-/-}; *Fzd6*^{-/-} double mutants, however, displayed a severe midbrain morphogenesis defect from the earliest stage (E10.5) analyzed, suggesting that these two receptors are involved in early morphogenetic processes required for the proper shaping of the anterior neural tube in the mouse embryo.

Fzd6 Does Not Transmit the Wnt1 Signal Required for MHB and mDA Neuron Development

We initially hypothesized that *Fzd6* might be a strong candidate to transduce the Wnt1 signal required for the establishment and maintenance of the IsO at the MHB, and for the proper development of mDA neurons, because of its striking expression at the MHB and in the caudal cephalic flexure. However, the analyses of the *Fzd6*^{-/-} single and *Fzd3*^{-/-}; *Fzd6*^{-/-} double mutants showed that this receptor is not involved in these processes. The expression of *Wnt1* or *Fgf8* was neither altered along the D/V and A/P axes of the neural tube nor developmentally regulated in the *Fzd6*^{-/-} and *Fzd3*^{-/-}; *Fzd6*^{-/-} embryos. Moreover, Th⁺ and Pitx3⁺ mDA neurons

arose normally in these mutants. Fzd6 is, therefore, unlikely to transmit the Wnt1 signal required for the proper development of the MHR and of mDA neurons. The analyses of the *Fzd3*^{-/-}; *Fzd6*^{+/-} and *Fzd3*^{-/-}; *Fzd6*^{-/-} embryos, however, revealed a previously unsuspected function of Fzd6 in early midbrain morphogenesis. Heterozygosity for *Fzd6* on an *Fzd3*^{-/-} background was sufficient to cause what appears to be an early neurulation defect. The contribution of Fzd6 to this phenotype is indeed enigmatic, given that *Fzd6* expression is initially (at E9.5) confined to small and defined regions in the anterior neural tube, and becomes even more restricted at later embryonic stages (Fischer et al., 2007). *Fzd6*, however, is strongly expressed in the mesenchyme surrounding the neural tube at these midgestational stages (Fischer et al., 2007). The identity of the cells or tissues within or outside the neural plate/tube expressing the Fzd6 receptor at earlier developmental stages and contributing to the double mutant phenotype, therefore, still needs to be established.

***Fzd3*^{-/-} Mutants Show a Transient Delay in mDA Neuron Differentiation: A Link to Schizophrenia?**

The ubiquitous expression of *Fzd3* in the mouse anterior neural tube and the severe axon outgrowth defects in the CNS of the *Fzd3*^{-/-} single mutants (Wang et al., 2002; Lyuksytova et al., 2003; Wang et al., 2006b; Fischer et al., 2007), made it another candidate to act either alone or redundantly with Fzd6 in the development of the MHR and of mDA neurons. The morphogenesis (including cell proliferation and survival) of the MHR and the generation of Pou4f1⁺ RN and tectal neurons, however, were not affected in the *Fzd3*^{-/-} embryos, suggesting a minor role of Fzd3 in the development of this region. Nevertheless, and despite an apparently normal expression of *Aldh1a1* and *Nr4a2* in their precursors at E10.5, the numbers of Th⁺ mDA neurons were conspicuously reduced in the *Fzd3*^{-/-} single mutants at E12.5. Although this reduction of Th⁺ mDA

neurons was only transient and appeared to recover already one day later in development, it suggested that the differentiation of *Aldh1a1*⁺ and *Nr4a2*⁺ mDA precursors into Th⁺ mDA neurons was delayed in the *Fzd3*^{-/-} mutants. In addition, we noted a transient medio-lateral broadening of the Th⁺/Pitx3⁺ mDA domain in the *Fzd3*^{-/-} embryos, that was most pronounced in the caudal midbrain and disappeared at approximately the same time when the Th⁺ mDA neuron numbers recovered in these mutants. At first sight, the mDA defect in the *Fzd3*^{-/-} embryos appears to resemble the phenotype of the *Wnt5a*^{-/-} mutants (Andersson et al., 2008). A closer look, however, reveals several differences between the *Fzd3*^{-/-} and *Wnt5a*^{-/-} mutant phenotype: first, the number of Th⁺ mDA neurons is transiently increased and not decreased in the *Wnt5a*^{-/-} mutants; second, proliferation in the FP region was also increased in the *Wnt5a*^{-/-} embryos; and third, the medio-lateral broadening of the mDA domain was most pronounced in the rostral and not in the caudal midbrain of the *Wnt5a*^{-/-} mutants and persisted throughout development (Andersson et al., 2008). As midbrain morphogenesis was also not altered in the *Fzd3*^{-/-} single mutants, in contrast to the *Wnt5a*^{-/-} mice (Andersson et al., 2008), it is unlikely that Fzd3 transduces the “non-canonical” Wnt5a/PCP signal. Remarkably, *Lrp6*^{-/-} mutants also display a transient delay in mDA neuron differentiation without any alterations in cell proliferation, survival, or midbrain patterning (Castelo-Branco et al., 2009, pages 211–221, this issue), thus resembling closely the *Fzd3*^{-/-} mutant phenotype. Moreover, the persistent reduction of Th⁺ mDA neuron numbers is a characteristic phenotype of other mouse mutants for the “canonical” Wnt1/β-catenin pathway (Prakash et al., 2006; Joksimovic et al., 2009; Tang et al., 2009), and *Xenopus* Fzd3 and Wnt1 strongly interact during neural crest development in the frog (Deardorff et al., 2001). The less severe and transient reduction of Th⁺ mDA neurons in the *Fzd3*^{-/-} and *Lrp6*^{-/-}X mutants, therefore, suggests that this receptor and co-receptor are involved in the

transduction of the Wnt1/β-catenin signal required for mDA neuron differentiation, but they might be functionally compensated by other Fzd/Lrp receptors/co-receptors during mouse development (see also the report by Castelo-Branco et al., 2009, pages 211–221, this issue).

The requirement of Fzd3 for the proper differentiation of mDA neurons in the mouse embryo, as described here, might also have some relevance for the pathogenesis of human neuropsychiatric disorders, in particular of schizophrenia. Polymorphisms in the human *FZD3* gene have been associated with schizophrenia, although these findings could not be replicated in all studies (reviewed by De Ferrari and Moon, 2006). The functional implications of these *FZD3* polymorphisms are still unclear, but it might now be hypothesized that apart from an aberrant neurotransmission due to the disruption of major fiber tracts (including the corticothalamic, thalamocortical and nigrostriatal pathways) (Wang et al., 2002, 2006b), a delayed differentiation of mDA neurons could also contribute to the pathogenesis of this disease in carriers of *FZD3* mutations.

Fzd3 and Fzd6 Control Midbrain Morphogenesis in the Mouse by an Unknown Mechanism

Our main finding is an improper morphogenesis of the early mouse brain in the *Fzd3*^{-/-}; *Fzd6*^{+/-} and *Fzd3*^{-/-}; *Fzd6*^{-/-} double mutants. This phenotype differs from the neural tube closure defects (exencephaly and craniorachischisis) reported before in the *Fzd3*^{-/-} single and *Fzd3*^{-/-}; *Fzd6*^{-/-} double mutants (Wang et al., 2002, 2006a). In fact, the anterior neural tube comprising fore-, mid-, and rostral hindbrain was properly closed in all (100%) double mutants at midgestation. The main defect consisted of a collapse of all brain ventricles leaving only a small gap between the neural tissues, and was observed at a penetrance of around 70% in the *Fzd3*^{-/-}; *Fzd6*^{-/-} embryos. This defect was already evident at E10.5 and was accompanied by a thickening of the neuroepithelium and of the overlying

mesenchyme in some regions, particularly in the dorsal MHR, that did not appear to be due to an increased proliferation in this region. Dorsal midbrain tissue had protruded and fused with ventrolateral tissues in some (43%) double mutants at E12.5, probably as a consequence of the focal disruption of the ventricular basal lamina and protrusion of individual cells into the remaining ventricular cavity of the midbrain observed at E10.5. These mutants also showed an increased proliferation in the DM and VM that might contribute to the occlusion of the mesencephalic (third) ventricle by the protruding neural tissue. The primary defect in the *Fzd3*^{-/-}; *Fzd6*^{+/-} and *Fzd3*^{-/-}; *Fzd6*^{-/-} double mutant brain is, therefore, not a neural tube closure defect, which is mainly characterized by the failure of neural fold elevation (Wallingford, 2005). It should be noted that apart from the proper elevation and fusion of the dorsal neural folds, the elongation (by convergent extension) of the neural tube, the formation of the median and dorsolateral hinge-points, and the orientation of neuroepithelial cells were not affected in the double mutant midbrain. These observations argue against a “classical” PCP or convergent extension phenotype in the *Fzd3*^{-/-}; *Fzd6*^{+/-} and *Fzd3*^{-/-}; *Fzd6*^{-/-} midbrain, characteristic for several mutants of the non-canonical Wnt/PCP pathway (Copp et al., 2003; Andersson et al., 2008). Moreover, expression of *Wnt1* and of one of its putative target genes, *Lmx1a*, along the A/P axis, and D/V patterning were not altered in the double mutant midbrain, indicating that patterning of the MHR proceeded independently of the morphogenetic defect. However, the analysis of earlier embryonic stages (at the beginning of neurulation) will be necessary to unravel the mechanism underlying the brain morphogenesis defect in the double mutants. At this point, we can only speculate about possible mechanisms: although neural fold elevation and fusion proceeds normally to form the neural tube, accompanying or subsequent cell migration and adhesion within the elevating neuroepithelium and/or within the surrounding mesenchyme might be aberrant in the double mutants. Alternatively or in addition, the ventricular cavities in the double mutant brain

might collapse as a consequence of a reduced or missing internal pressure due to the closure defect in the caudal neural tube of the *Fzd3*^{-/-}; *Fzd6*^{+/-} and *Fzd3*^{-/-}; *Fzd6*^{-/-} embryos.

The molecular details of Fzd3 and Fzd6 function in mouse brain morphogenesis are completely unknown and remain to be investigated, but their involvement in midbrain morphogenesis is somewhat enigmatic for the following reason. Neither single mutant displays a midbrain morphogenesis defect, but a reduction of *Fzd6* gene dosage in the complete absence of *Fzd3* was sufficient to cause this defect, albeit at a reduced penetrance. This suggests a redundant function of Fzd3 and Fzd6, together with other (unknown) genetic modifiers. Expression of these two receptors, however, is mostly confined to two different compartments in the midgestational mouse head: Fzd3 is strongly expressed in the neuroepithelium of the anterior neural tube and only very weakly in the surrounding mesenchyme, whereas Fzd6 expression is strongest in the surrounding mesenchyme and highly restricted and weaker in the anterior neural tube (Fischer et al., 2007). Moreover, our data suggest a participation of Fzd3 in the transduction of the Wnt1/β-catenin signal required for mDA neuron development in the VM, whereas the human FZD6 receptor was reported to transmit a signal antagonizing the canonical Wnt/β-catenin pathway (Golan et al., 2004). It, therefore, remains to be established whether Fzd3 and Fzd6 cooperate within the same pathway, as implied by previous reports (Wang et al., 2002, 2006a; Guo et al., 2004), or act in antagonistic pathways during midbrain morphogenesis. Alternatively, these two Fzd molecules might operate independently of any Wnt signals in the morphogenesis of the early mouse brain (Seifert and Mlodzik, 2007; van Amerongen et al., 2008).

EXPERIMENTAL PROCEDURES

Mutant Mice

Outbred CD-1 mice were purchased from Charles River (Kisslegg/Germany). Generation and genotyping

of *Fzd3*^{-/-} and *Fzd6*^{-/-} mice was described by Wang et al. (2002) and Guo et al. (2004). Mutant mouse lines were maintained on a mixed C57BL/6 × 129/SVJ background (Wang et al., 2006a). Male *Fzd3*^{+/-}; *Fzd6*^{-/-} mice were reported to have a strongly reduced fertility, but in our hands, male *Fzd3*^{+/-}; *Fzd6*^{-/-} mice did not produce any sperm at all (data not shown), although we kept the same genetic background as Wang et al. (2006a). The infertility of our male *Fzd3*^{+/-}; *Fzd6*^{-/-} mice forced us to change our breeding scheme and to use double heterozygote *Fzd3*^{+/-}; *Fzd6*^{+/-} males intercrossed with *Fzd3*^{+/-}; *Fzd6*^{+/-} or *Fzd3*^{+/-}; *Fzd6*^{-/-} females. *Fzd3*^{-/-}; *Fzd6*^{-/-} double mutant embryos were obtained by natural matings or by in vitro fertilization according to standard procedures. *Fzd3*^{+/+}; *Fzd6*^{-/-} and *Fzd3*^{+/-}; *Fzd6*^{+/-} embryos were used as “wild-type” controls as these embryos do not display a neural tube phenotype (this report; Wang et al., 2006a). Collection of embryonic stages was done from timed-pregnant females as indicated in the text. Noon of the day of vaginal plug detection was designated embryonic day (E) 0.5. Animal treatment was conducted under federal guidelines for the use and care of laboratory animals and was approved by the HMGU Institutional Animal Care and Use Committee.

Radioactive In Situ Hybridization (ISH) and Immunohistochemistry

Paraffin sections (8 μm) of mouse embryos were processed for radioactive ISH or for immunohistochemistry as described in Prakash et al. (2006) and Fischer et al. (2007). Riboprobes for *Fzd6*, *Wnt1*, *Aldh1a1*, *Th*, *Fgf8*, *Nr4a2*, *Dat*, *Lmx1a*, and *Lmx1b* were reported by a number of authors (Niederreither et al., 2002; Brodski et al., 2003; Puelles et al., 2003; Fischer et al., 2007; Prakash et al., 2009). Monoclonal antibodies used were mouse Th (1:600; Chemicon), Pou4f1 (Brn3a) (1:100; Santa Cruz Biotechnology), Nkx2-2 (1:100), Pax7 (1:50) (both obtained from the Developmental Studies Hybridoma Bank developed under the auspices of the

NICHD and maintained by The University of Iowa, Department of Biology, Iowa City, IA 52242), p27^{Kip1} (Cdkn1b) (1:2,000; BD Transduction Laboratories), Ascl1 (Mash1) (1:40; BD Pharmingen) and NeuN (1:300; Chemicon), rat BrdU (1:100; AbD Serotec), and rabbit-cleaved Caspase 3 (cCasp3) (1:100; Cell Signaling). Polyclonal antisera used were rabbit Th (1:150; Chemicon), Pitx3 (1:300; Zymed/Invitrogen), phosphorylated Histone H3 (pH3) (1:500; Upstate), Dbx1 (1:5,000; gift from A. Pierani), cyclin D1 (Cnd1) (1:150; Thermo Scientific) and Sox2 (1:200; Santa Cruz Biotechnology), and guinea pig Nkx6-2 (1:5,000; gift from J. Ericson). Secondary antibodies (donkey anti-mouse, -rat, -rabbit, and -guinea pig) were either fluorescently labeled (Cy3, Jackson ImmunoResearch; AlexaFluor 488 and 594, Molecular Probes), or coupled to biotin/streptavidin-horseradish-peroxidase (Jackson ImmunoResearch) and detected using the Vectastain ABC System (Vector Laboratories). Brightfield, darkfield, and fluorescent images were taken on an Axioplan2 or Axiovert 200M microscope and StemiSV6 stereomicroscope equipped with AxioCam MRc or HRc camera (Zeiss), or on a confocal laser scanning microscope (LSM 510 META, Zeiss). Images were processed with AxioVision 4.6 (Zeiss) and Adobe Photoshop CS3 (Adobe Systems Inc.) software.

5-Bromo-2'-Deoxyuridine (BrdU) Treatments

Pregnant dams were injected intraperitoneally with 10 μ g BrdU (Sigma)/g body weight on E10.5 or E12.5. Embryos were dissected 2 hr later and processed for immunodetection of BrdU.

Unbiased Stereology, Cell Countings, and Length Measurements

Th⁺ and Pitx3⁺ cells were evaluated by the optical fractionator method, and BrdU⁺ and pH3⁺ cells were counted using the StereoInvestigator 5.05.4 software (MBF Bioscience, Williston, VT) on every sixth section from serial coronal paraffin sections (8 μ m) through the midbrain of E10.5, E11.5,

E12.5, E13.5, and E17.5 embryos. The D/V and left-right (lateral) extension of the midbrain was measured on 4 consecutive Nissl-stained paraffin sections from E12.5 embryos using AxioVisionLE (Zeiss) software.

Statistical Analyses

For comparisons between wild-type and mutant animals from the same litters, methods for paired or grouped data were applied, namely the paired *t*-test and repeated-measurements ANOVA. Repeated-measurements methods were also applied for comparisons between wild-type and mutant embryos with several sections per embryo. For analysis of the effect of two factors simultaneously, first a two-way ANOVA with interaction was fitted. If the interaction effect was significant, one-way ANOVAs were performed for subgroups. Otherwise a two-way ANOVA without interaction effect was fitted. In case of a significant genotype effect, post-hoc one-way ANOVAs with *P* value correction according to HOLM were calculated to assess the genotype effect in subgroups (Holm, 1979). For all calculations, the R software with the nlme package was used (Pinheiro et al., 2008; R Development CoreTeam, 2008).

ACKNOWLEDGMENTS

The authors thank J. Nathans for providing the *Fzd3* and *Fzd6* mutant mice, A. Pierani and J. Ericson for antibodies, A. Simeone for discussions, and S. Laass for excellent technical assistance. This work was funded by the Federal Ministry of Education and Research (BMBF) in the framework of the National Genome Research Network (NGFN+ Functional Genomics of Parkinson Disease FKZ 01GS08174), by Virtual Institute on Neurodegeneration and Ageing (VH-VI-252), by the Initiative and Networking Fund in the framework of the Helmholtz Alliance of Systems Biology and of Mental Health in an Ageing Society (HA-215), Bayerischer Forschungsverbund "ForNeuroCell" (F2-F2410-10c/20697), European Union (mdDANEURODEV FP7-Health-2007-B-222999, EuTRACC LSHG-CT-2006-037445), and Deutsche For-

schungsgemeinschaft (DFG) SFB 596, WU 164/3-2, and WU 164/4-1.

REFERENCES

- Andersson E, Tryggvason U, Deng Q, Friling S, Alekseenko Z, Robert B, Perlmann T, Ericson J. 2006. Identification of intrinsic determinants of midbrain dopamine neurons. *Cell* 124:393–405.
- Andersson ER, Prakash N, Cajanek L, Minina E, Bryja V, Bryjova L, Yamaguchi TP, Hall AC, Wurst W, Arenas E. 2008. Wnt5a regulates ventral midbrain morphogenesis and the development of A9-A10 dopaminergic cells in vivo. *PLoS ONE* 3:e3517.
- Ang S-L. 2006. Transcriptional control of midbrain dopaminergic neuron development. *Development* 133:3499–3506.
- Brault V, Moore R, Kutsch S, Ishibashi M, Rowitch DH, McMahon AP, Sommer L, Boussadia O, Kemler R. 2001. Inactivation of the beta-catenin gene by Wnt1-Cre-mediated deletion results in dramatic brain malformation and failure of craniofacial development. *Development* 128:1253–1264.
- Brodski C, Weisenhorn DM, Signore M, Silaber I, Oesterheld M, Broccoli V, Acampora D, Simeone A, Wurst W. 2003. Location and size of dopaminergic and serotonergic cell populations are controlled by the position of the midbrain-hindbrain organizer. *J Neurosci* 23:4199–4207.
- Castelo-Branco G, Andersson ER, Minina E, Sousa KM, Ribeiro D, Kokubu C, Imai K, Prakash N, Wurst W, Arenas E. 2009. Delayed dopaminergic neuron differentiation in *Lrp6* mutant mice. *Dev Dyn* 239:211–221.
- Chizhikov VV, Millen KJ. 2004a. Control of roof plate development and signaling by Lmx1b in the caudal vertebrate CNS. *J Neurosci* 24:5694–5703.
- Chizhikov VV, Millen KJ. 2004b. Control of roof plate formation by Lmx1a in the developing spinal cord. *Development* 131:2693–2705.
- Copp AJ, Greene NDE, Murdoch JN. 2003. Dishevelled: linking convergent extension with neural tube closure. *Trends Neurosci* 26:453–455.
- De Ferrari GV, Moon RT. 2006. The ups and downs of Wnt signaling in prevalent neurological disorders. *Oncogene* 25:7545–7553.
- Deardorff MA, Tan C, Saint-Jeannet JP, Klein PS. 2001. A role for frizzled 3 in neural crest development. *Development* 128:3655–3663.
- Fedtsova NG, Turner EE. 1995. Brn-3.0 expression identifies early post-mitotic CNS neurons and sensory neural precursors. *Mech Dev* 53:291–304.
- Fischer T, Guimera J, Wurst W, Prakash N. 2007. Distinct but redundant expression of the Frizzled Wnt receptor genes at signaling centers of the developing mouse brain. *Neuroscience* 147:693–711.
- Gates MA, Torres EM, White A, Fricker-Gates RA, Dunnett SB. 2006. Re-

- examining the ontogeny of substantia nigra dopamine neurons. *Eur J Neurosci* 23:1384–1390.
- Golan T, Yaniv A, Bafico A, Liu G, Gazit A. 2004. The human Frizzled 6 (HFz6) acts as a negative regulator of the canonical Wnt/ β -catenin signaling cascade. *J Biol Chem* 279:14879–14888.
- Guo N, Hawkins C, Nathans J. 2004. Frizzled6 controls hair patterning in mice. *Proc Natl Acad Sci USA* 101:9277–9281.
- Holm S. 1979. A simple sequentially rejective multiple test procedure. *Scand. J Statistics* 6:65–70.
- Huang H, He X. 2008. Wnt/ β -catenin signaling: new (and old) players and new insights. *Curr Opin Cell Biol* 20:119–125.
- Huang HC, Klein PS. 2004. The Frizzled family: receptors for multiple signal transduction pathways. *Genome Biol* 5:234.231–234.237.
- Ille F, Sommer L. 2005. Wnt signaling: multiple functions in neural development. *Cell Mol Life Sci* 62:1–9.
- Joksimovic M, Yun BA, Kittappa R, Anderegg AM, Chang WW, Taketo MM, McKay RD, Awatramani RB. 2009. Wnt antagonism of Shh facilitates midbrain floor plate neurogenesis. *Nat Neurosci* 12:125–131.
- Kele J, Simplicio N, Ferri ALM, Mira H, Guillemot F, Arenas E, Ang S-L. 2006. Neurogenin 2 is required for the development of ventral midbrain dopaminergic neurons. *Development* 133:495–505.
- Kittappa R, Chang WW, Awatramani RB, McKay RDG. 2007. The *foxa2* gene controls the birth and spontaneous degeneration of dopamine neurons in old age. *PLoS Biol* 5:e325.
- Logan CY, Nusse R. 2004. The Wnt signaling pathway in development and disease. *Annu Rev Cell Dev Biol* 20:781–810.
- Lyuksyutova AI, Lu CC, Milanese N, King LA, Guo N, Wang Y, Nathans J, Tessier-Lavigne M, Zou Y. 2003. Anterior-posterior guidance of commissural axons by Wnt-frizzled signaling. *Science* 302:1984–1988.
- Martinez S. 2001. The isthmic organizer and brain regionalization. *Int J Dev Biol* 45:367–371.
- McMahon AP, Bradley A. 1990. The Wnt-1 (*int-1*) proto-oncogene is required for development of a large region of the mouse brain. *Cell* 62:1073–1085.
- Megason SG, McMahon AP. 2002. A mitogen gradient of dorsal midline Wnts organizes growth in the CNS. *Development* 129:2087–2098.
- Millonig JH, Millen KJ, Hatten ME. 2000. The mouse Dreher gene *Lmx1a* controls formation of the roof plate in the vertebrate CNS. *Nature* 403:764–769.
- Nakatani T, Minaki Y, Kumai M, Ono Y. 2007. Helt determines GABAergic over glutamatergic neuronal fate by repressing *Ngn* genes in the developing mesencephalon. *Development* 134:2783–2793.
- Niederreither K, Fraulob V, Garnier J-M, Chambon P, Dolle P. 2002. Differential expression of retinoic acid-synthesizing (RALDH) enzymes during fetal development and organ differentiation in the mouse. *Mech Dev* 110:165–171.
- Ono Y, Nakatani T, Sakamoto Y, Mizuhara E, Minaki Y, Kumai M, Hamaguchi A, Nishimura M, Inoue Y, Hayashi H, Takahashi J, Imai T. 2007. Differences in neurogenic potential in floor plate cells along an anteroposterior location: midbrain dopaminergic neurons originate from mesencephalic floor plate cells. *Development* 134:3213–3225.
- Perlmann T, Wallen-Mackenzie A. 2004. *Nurr1*, an orphan nuclear receptor with essential functions in developing dopamine cells. *Cell Tissue Res* 318:45–52.
- Pinheiro J, Bates D, DebRoy S, Sarkar D, R Core team. 2008. nlme: Linear and Nonlinear Mixed Effects Models. R package version 3.1–89.
- Prakash N, Brodski C, Naserke T, Puelles E, Gogoi R, Hall A, Panhuysen M, Echevarria D, Sussel L, Weisenhorn DMV, Martinez S, Arenas E, Simeone A, Wurst W. 2006. A Wnt1-regulated genetic network controls the identity and fate of midbrain-dopaminergic progenitors in vivo. *Development* 133:89–98.
- Prakash N, Puelles E, Freude K, Trumbach D, Omodei D, Di Salvio M, Sussel L, Ericson J, Sander M, Simeone A, Wurst W. 2009. *Nkx6-1* controls the identity and fate of red nucleus and oculomotor neurons in the mouse midbrain. *Development* 136:2545–2555.
- Puelles E, Acampora D, Lacroix E, Signore M, Annino A, Tuorto F, Filosa S, Corte G, Wurst W, Ang SL, Simeone A. 2003. Otx dose-dependent integrated control of antero-posterior and dorso-ventral patterning of midbrain. *Nat Neurosci* 6:453–460.
- R Development Core Team 2008. R: A language and environment for statistical computing. Vienna, Austria: R Foundation for Statistical Computing.
- Seifert JR, Mlodzik M. 2007. Frizzled/PCP signalling: a conserved mechanism regulating cell polarity and directed motility. *Nat Rev Genet* 8:126–138.
- Smidt MP, Asbreuk CH, Cox JJ, Chen H, Johnson RL, Burbach JP. 2000. A second independent pathway for development of mesencephalic dopaminergic neurons requires *Lmx1b*. *Nat Neurosci* 3:337–341.
- Smidt MP, Smits SM, Burbach JPH. 2004. Homeobox gene *Pitx3* and its role in the development of dopamine neurons of the substantia nigra. *Cell Tissue Res* 318:35–43.
- Tang M, Miyamoto Y, Huang EJ. 2009. Multiple roles of β -catenin in controlling the neurogenic niche for midbrain dopamine neurons. *Development* 136:2027–2038.
- Thomas KR, Capecchi MR. 1990. Targeted disruption of the murine *int-1* proto-oncogene resulting in severe abnormalities in midbrain and cerebellar development. *Nature* 346:847–850.
- van Amerongen R, Mikels A, Nusse R. 2008. Alternative wnt signaling is initiated by distinct receptors. *Sci Signal* 1:re9.
- Wallen A, Zetterstrom RH, Solomin L, Arvidsson M, Olson L, Perlmann T. 1999. Fate of mesencephalic AHD2-expressing dopamine progenitor cells in *Nurr1* mutant mice. *Exp Cell Res* 253:737–746.
- Wallingford JB. 2005. Neural tube closure and neural tube defects: Studies in animal models reveal known knowns and known unknowns. *Am J Med Genet C Semin Med Genet* 135C:59–68.
- Wang Y, Thekdi N, Smallwood PM, Macke JP, Nathans J. 2002. Frizzled-3 is required for the development of major fiber tracts in the rostral CNS. *J Neurosci* 22:8563–8573.
- Wang Y, Guo N, Nathans J. 2006a. The role of Frizzled3 and Frizzled6 in neural tube closure and in the planar polarity of inner-ear sensory hair cells. *J Neurosci* 26:2147–2156.
- Wang Y, Zhang J, Mori S, Nathans J. 2006b. Axonal growth and guidance defects in Frizzled3 knock-out mice: a comparison of diffusion tensor magnetic resonance imaging, neuro filament staining, and genetically directed cell labeling. *J Neurosci* 26:355–364.
- Wilkinson DG, Bailes JA, McMahon AP. 1987. Expression of the proto-oncogene *int-1* is restricted to specific neural cells in the developing mouse embryo. *Cell* 50:79–88.
- Wurst W, Bally-Cuif L. 2001. Neural plate patterning: upstream and downstream of the isthmic organizer. *Nat Rev Neurosci* 2:99–108.
- Zervas M, Millet S, Ahn S, Joyner AL. 2004. Cell behaviors and genetic lineages of the mesencephalon and rhombomere 1. *Neuron* 43:345–357.